

1 **Supplemental Material**

2 **Supplemental Materials and Methods:**

3 **Cell lines**

4 The MM cell line MM1.S, mantle cell lymphoma cell line JeKo-1, T cell lymphoma cell  
5 line Jurkat, chronic myelogenous leukemia cell line K562, and fibroblast cell line WI-  
6 38 were purchased from ATCC, Manassas, VA, USA, and the MM cell line OPM-2 was  
7 purchased from DSMZ, Braunschweig, Germany. The MM cell line ALMC-2 was gifted  
8 by Dr. Diane Jelinek. The mouse melanoma cell line B16 was gifted by Dr. Michael  
9 Barry. These cell lines were transduced with a luciferase-ZsGreen lentivirus (Addgene,  
10 Cambridge, MA, USA) and sorted to 100% purity, as previously described<sup>1,2</sup>. Cell lines  
11 were cultured in R10 medium made with Roswell Park Memorial Institute (RPMI) 1640  
12 (Gibco, Gaithersburg, MD, USA), 10% Fetal Bovine Serum (FBS, Sigma, St. Louis,  
13 MO, USA), and 1% Penicillin-Streptomycin-Glutamine (Gibco, Gaithersburg, MD,  
14 USA). Flow cytometric analysis of SLAMF7 expression on MM1.S, OPM-2, ALMC-2  
15 cells showed similar pattern (Supplemental Figure S13). All cell lines used were  
16 regularly tested negative for mycoplasma contamination throughout the whole  
17 duration of this study.

18

19 **Multi-parametric flow cytometry**

20 Anti-human antibodies were purchased from Biolegend, eBioscience, or BD  
21 Biosciences (San Diego, CA, USA). The preparation of samples for flow cytometry  
22 was described previously<sup>2</sup>. Countbright beads (Invitrogen, Carlsbad, CA, USA) were  
23 used for cell number quantitation, as previously described<sup>2</sup>.

24 A goat anti-mouse F(ab') antibody (Invitrogen, Carlsbad, CA, USA) was used for  
25 detecting a single transduced BCMA, SLAMF7, or FAP CAR. To assess dual  
26 transduced CARs, labelled proteins for the specific CAR were used. For BCMA CAR,  
27 human BCMA/TNFRSF17 protein, Fc Tag (BC7-H5254-100ug, ACRO Biosystems,  
28 Newark, DE) was used for primary staining, followed by Alexa Fluor 647-conjugated  
29 anti-human IgG Fc antibody (109-606-170, Jackson ImmunoResearch, West Grove,  
30 PA). For SLAMF7 CAR and FAP CAR staining, human SLAMF7/CRACC/CD319  
31 protein, His Tag (SL7-H5225-100ug, ACRO Biosystems, Newark, DE) or  
32 recombinant human FAP, His tagged (FAP-1141H, Creative BioMart, Shirley, NY)  
33 was used for primary staining, respectively, followed by FITC conjugated anti-6X His  
34 tag antibody (Cambridge, CB2 0AX, UK). The following antibodies were also used:  
35 anti-human CD45 (clone HI30) BV421 (cat# 304032, BioLegend, San Diego, CA,  
36 USA), anti-mouse CD45 (clone 30-F11) APC- eFluor 780 (cat# 103116, BioLegend,  
37 San Diego, CA, USA), CD3 (clone UCHT1) PE-Cy7 (cat# 300420, BioLegend, San  
38 Diego, CA, USA), CD3 (clone UCHT1) APC (cat# 17-0038-42, eBiosciences, San  
39 Diego, CA, USA), and CD3 (clone SK7) APC-H7 (cat# 560176, BD Pharmingen, San  
40 Diego, CA, USA), CD107a (clone H4A3) FITC (cat# 555800, BD Pharmingen, San  
41 Diego, CA, USA), IL-2 (clone 5344.111) PE-CF594 (cat# 562384, BD Pharmingen,  
42 San Diego, CA, USA), GM-CSF (clone BVD2-21C11) BV421 (cat# 562930, BD  
43 Pharmingen, San Diego, CA, USA), IFN- $\gamma$  (clone 4S.B3) APC-eFluor 780 (cat# 47-  
44 7319-42, Invitrogen, Carlsbad, CA, USA), MIP1- $\beta$  (clone D21-1351) PE-Cy7 (cat#  
45 560687, BD Pharmingen, San Diego, CA, USA), BCMA (clone 19F2) PE-Cy7 (cat#  
46 357507, BioLegend, San Diego, CA, USA), SLAMF7 (clone 162) PE (cat# 12-2229-

47 42, Invitrogen, Carlsbad, CA, USA), SLAMF7 (clone 162) APC (cat# 331809,  
48 BioLegend, San Diego, CA, USA), FAP (clone 427819) PE (cat# FAB3715P-025,  
49 R&D Systems, Minneapolis, MN, USA), SMA (clone 1A4) APC (cat# IC1420A, R&D  
50 Systems, Minneapolis, MN, USA), human CD45 (clone 2D1) PerCP (cat# 340665,  
51 BD Pharmingen, San Diego, CA, USA), PD-1 (clone EH12.2H7) BV421 (cat#  
52 329920, BioLegend, San Diego, CA, USA), PD-L1 (clone 29E.2A3) BV421 (cat#  
53 329714, BioLegend, San Diego, CA, USA). For murine FAP staining, rat anti-mouse  
54 FAP (clone 983802) (cat# MAB9727, R&D Systems, Minneapolis, MN, USA),  
55 followed by phycoerythrin-conjugated anti-rat IgG secondary antibody (cat# F0105B,  
56 R&D Systems, Minneapolis, MN, USA). For murine SLAMF7 staining, rat anti-mouse  
57 SLAMF7 (clone 983802) (cat# MAB46281, R&D Systems, Minneapolis, MN, USA),  
58 followed by phycoerythrin-conjugated anti-rat IgG secondary antibody. Flow  
59 cytometry was performed on three-laser CytoFLEX (Beckman Coulter, Chaska, MN,  
60 USA). All analyses were performed using FlowJo X10.0.7r2 software (Ashland, OR,  
61 USA).

62

### 63 **Bone marrow-derived mesenchymal stem cells (BM-MSCs)**

64 BM-MSCs were obtained under a Mayo Clinic IRB approved protocol (IRB# 1062-  
65 00). Whole normal bone marrow aspirates from patients with nonmalignant disease  
66 which requires an orthopedic procedure (e.g. hip replacement) resulting in waste of  
67 normal bone marrow. Samples are only identified with a laboratory assigned  
68 sequence number. Whole bone marrow aspirates were first filtered through a 70 µm  
69 nylon cell strainer (Falcon/Corning Inc., cat.# 352350). To lyse the red blood cells

70 (RBCs), ACK lyse buffer was added to the bone marrow samples. MEM-alpha  
71 medium was used to culture bone marrow samples. Once confluent, supernatant  
72 was discarded, and adherent cells were trypsinized and cryopreserved.

73

#### 74 **Primary cells and CART cells**

75 The use of recombinant DNA in the laboratory was approved by the Mayo Clinic  
76 Institutional Biosafety Committee (IBC), IBC number HIP00000252.20. Peripheral  
77 blood mononuclear cells (PBMC) were isolated from de-identified normal donor  
78 blood apheresis cones obtained under a Mayo Clinic IRB approved protocol, using  
79 SepMate tubes (STEMCELL Technologies, Vancouver, Canada). T cells were  
80 separated with negative selection magnetic beads using EasySep™ Human T Cell  
81 Isolation Kit (STEMCELL Technologies). Second generation BCMA, SLAMF7, or  
82 FAP CAR constructs were synthesized *de novo* (IDT, Coralville, IA, USA) and cloned  
83 into a third-generation lentivirus under the control of the EF-1 $\alpha$  promoter. Several  
84 constructs were synthesized using different co-stimulation as indicated below and in  
85 the described specific experiments. The BCMA CAR construct (C11D5.3-41BBz)  
86 included 4-1BB costimulation and a single chain variable fragment (scFv) derived  
87 from an anti-human BCMA antibody clone C11D5.3<sup>3</sup>. The SLAMF7 CAR construct  
88 (Luc90-CD28z) included CD28 costimulation and an scFv derived from a mouse  
89 anti-human SLAMF7 antibody clone Luc90<sup>4,5</sup>. The FAP CAR construct (FAP05-  
90 41BBz) included 4-1BB costimulation and an scFv derived from anti-FAP clone FAP-  
91 05. These constructs are presented in Supplemental Figure S14A. BCMA, SLAMF7,  
92 or FAP CART cells were then generated through the lentiviral transduction of normal

93 donor T cells. The generation of lentiviral particles was described previously<sup>2</sup>. The  
94 titers and subsequently multiplicity of infection (MOI) were analyzed and calculated  
95 by flow cytometry as described previously<sup>2</sup>. T cells isolated from normal donors were  
96 stimulated using Cell Therapy Systems Dynabeads CD3/CD28 (Life Technologies,  
97 Oslo, Norway) at a 1:3 ratio (cells:beads) and then transduced 24 hours after  
98 stimulation with lentivirus particles at a MOI of 5.0. Magnetic bead removal and the  
99 evaluation of CAR expression on T cells by flow cytometry were performed on day 6.  
100 The representative flow plots of CART cells are shown in Supplemental Figure  
101 S14B. CART cells were harvested and cryopreserved on day 8 for future  
102 experiments. CART cells were thawed and rested in T cell medium 6-12 hours prior  
103 to their use in experiments, as specified in each experiment.

104

105 **RNA isolation and reverse transcription-quantitative polymerase chain**  
106 **reaction (RT-qPCR)**

107 Total RNAs were extracted with QIAzol lysis reagent (Qiagen, Hilden, Germany) and  
108 miRNeasy Micro Kit Reagent (Qiagen) according to the manufacturer's protocol. RT-  
109 qPCR analysis of BCMA, SLAMF7, and FAP was performed with 1 µg of total RNA  
110 and iScript Advanced cDNA Synthesis Kit for RT-qPCR (Bio-Rad, Hercules,  
111 California, USA). The primer sequences used were as follows: BCMA forward primer,  
112 5'-TGTTCTTCTAATACTCCTCCTCT-3' and reverse primer, 5'-  
113 AACTCGTCCTTTAATGGTTC-3'; SLAMF7 forward primer, 5'-  
114 AGCAGCCCTCCACCCAGGAG-3' and reverse primer, 5'-  
115 AGGGCCTTCCAGGTATAAATCAC-3'; and FAP forward primer, 5'-

116 GGAAGTGCCTGTTCCAGCAATG-3' and reverse primer, 5'-  
117 TGTCTGCCAGTCTTCCCTGAAG-3'. Primers specific for TBP forward, 5'-  
118 GCCAGCTTCGGAGAGTTCTGGGATT-3' and reverse, 5'-  
119 CGGGCACGAAGTGCAATGGTCTTTA-3'). RT-qPCR was performed in an S1000  
120 Thermal Cycler (Bio-Rad). PCR conditions consisted of the following: 95°C for 3 min  
121 for denaturation; 95°C for 30 sec for annealing; and 62°C for 20 sec for extension,  
122 for 49 cycles. The threshold cycle for each sample was selected from the linear  
123 range and converted to a starting quantity by interpolation from a standard curve  
124 generated on the same plate for each set of primers. The BCMA, SLAMF7, and FAP  
125 messenger (m) RNA levels were normalized for each well to the TBP mRNA levels  
126 using the  $2^{-\Delta\Delta Cq}$  method.

127

## 128 **Immunohistochemistry**

129 The bone marrow samples were harvested, fixed and embedded in paraffin. The  
130 blocks were sliced into 5 mm sections and then dewaxed by zylene. The slides were  
131 dehydrated using increasing concentrations of alcohol. The sections were  
132 immunostained with primary antibodies: anti-CD3 (clone LN10, Leica Biosystems,  
133 Buffalo Grove, IL), anti-CD138 (clone MI15, Leica Biosystems), anti-FSP-1 (clone  
134 15E2E2, Millipore Sigma) followed by reaction with BOND Polymer Refine Detection  
135 Kit (Leica Biosystems). Images were taken of at least three randomly selected fields  
136 per sample. Percentage of FSP-1-positive area by calculating the ratio of positive  
137 staining area to total area using ImageJ software (National Institute of Health).

138 **Statistics**

139 Prism Graph Pad (La Jolla, CA, USA) and Microsoft Excel (Microsoft, Redmond,  
140 WA, USA) were used to analyze the experimental data. The high cytokine  
141 concentrations in the heat map were normalized to “1” and low concentrations  
142 normalized to “0” via Prism. Statistical tests are described in the figure legends.  
143 Briefly, normally distributed data were tested by one- and two-way analysis of  
144 variance (ANOVA) followed by Dunnett’s multiple comparisons test, and unpaired  
145 and paired two-sample Student’s *t*-test or Mann–Whitney U test for two-group  
146 comparisons. Log-rank test was used to test the hypotheses for *in vivo* survival.

147 **Supplemental Figure Legends**

148 **Supplemental Figure S1 | Potent anti-tumor activity of BCMA-CART cells against**

149 **BCMA expressing cells *in vitro*. A,** BCMA-CART-cells were co-cultured at different

150 E:T ratios with luciferase<sup>+</sup> MM1.S. At 24 hours, cell killing was assessed by

151 luminescence relative to controls (\*\*\*\* p<0.0001, two-way ANOVA; n=3, 2 replicates).

152 **B,** CFSE-labeled BCMA-CART were co-cultured with lethally irradiated MM1.S for 5

153 days. Cells were then analyzed for CFSE dilution to detect cell proliferation, and

154 absolute number of CART cells was counted by flow cytometry (5 ng/mL phorbol 12-

155 myristate 13-acetate (PMA) and 0.1 µg/mL ionomycin stimulation was used as a

156 positive control; n=3, 2 replicates). **C,** BCMA-CART-cells exhibited more antigen-

157 specific proliferation compared to untransduced T cells (UTD). BCMA-CART or UTD

158 derived from the same donor were co-cultured with lethally irradiated MM1.S for 5

159 days. Antigen-specific proliferation was measured by flow cytometry after 5 days using

160 absolute counts with counting beads. **D,** BCMA-CART or UTD were co-cultured with

161 lethally irradiated K562, MM1.S, or OPM-2 cells for 5 days. Absolute number of T cells

162 were counted via flow cytometry (mean and SEM, \*\*\*\* p<0.0001, one-way ANOVA;

163 n=3, 2 replicates). **E,** BCMA-CART cell degranulation and cytokine release assay.

164 BCMA-CART degranulation assay and cytokine production. BCMA-CART or UTD

165 were co-cultured with MM1.S for 4 hours. Medium was used as a negative control

166 (mean and SEM, \*\*\*\*p<0.0001, \*\*p<0.005, one-way ANOVA; n=3, 2 replicates). **F,**

167 Representative flow plots of BCMA-CART or UTD CD107a degranulation and

168 intracellular cytokine assays.



169 **Supplemental Figure S2 | Potent anti-tumor activity of BCMA-CART-cells against**  
170 **BCMA-expressing cells *in vivo*. A**, Experimental schema of BCMA-CART-cells in  
171 MM xenograft model. NSG mice were engrafted with luciferase<sup>+</sup>OPM-2 (1x10<sup>6</sup>  
172 cells/mouse, IV, 6 mice per group). On day 28, mice were randomized according to  
173 tumor burden, which was accessed by BLI, to receive 1x10<sup>6</sup> UTD, 1x10<sup>6</sup> BCMA-CART-  
174 cells, 0.5x10<sup>6</sup> BCMA-CART-cells, or 0.25x10<sup>6</sup> BCMA-CART-cells. **B**, BLI curve of *in*-  
175 *vivo* BCMA-CART-cell dose-finding assay. **C-D**, Anti-myeloma activity of BCMA-  
176 CART-cells in OPM-2 xenograft mice, which was shown by bioluminescence imaging  
177 (mean and SEM, \*\*p=0.006 at day 21, unpaired, two-sided, Student's t-test). **E**,  
178 Kaplan-Meier survival curve is shown [hazard ratio = 0.03320; 95% confidence interval  
179 (CI) = 0.004605 to 0.2393, \*\*\*p=0.0007, log-rank test]. **F**, Immunohistochemical  
180 analysis of BM samples harvested from OPM-2 xenograft mice treated with BCMA-  
181 CART-cells (magnification 10). **G**, Immunohistochemical analysis of bone marrow from  
182 OPM-2 xenograft models, which were treated with UTD (H&E, *upper left and right*,  
183 magnification 10 and 40, respectively. CD138, *lower left*, magnification 10), and FSP-  
184 1 (*lower right*) staining revealed the absence of BM-CAFs in this model.

185

186 **Supplemental Figure S3 | Bone marrow-derived cancer-associated fibroblasts**  
187 **(BM-CAFs) accelerate MM1.S cell growth *in vivo*.** NSG mice were intravenously  
188 injected with 1x10<sup>6</sup> of luciferase<sup>+</sup> MM1.S cells or in combination with 1x10<sup>6</sup> of BM-  
189 CAFs. Tumor growth was assessed with a bioluminescence imager (mean and SEM,  
190 \*\*\*\* p<0.0001, two-way ANOVA; n=3).

191

192 **Supplemental Figure S4 | BM-CAFs inhibit BCMA-CART effector functions. A,**  
193 CFSE-labeled BCMA-CART or UTD were co-cultured with lethally irradiated  
194 BCMA<sup>+</sup>SLAMF7<sup>+</sup>MM1.S and BM-CAFs for 5 days (mean and SEM, \*\*\*\*p<0.0001, two-  
195 way ANOVA; n=3, 2 replicates). **B,** Antigen-specific BCMA-CART CD107a  
196 degranulation assay in the presence of BM-CAFs. OPM-2 cells were used as a  
197 stimulator (\*\*p<0.01, unpaired, two-sided, Student's t-test; n=3, 2 replicates). **C,** CTLA-  
198 4 expression on BCMA-CART in the presence or absence of CAFs (Student's t-test;  
199 n=3, 2 replicates). **D,** Representative flow plots of surface PD-1 expression on BCMA-  
200 CART cells when co-cultured with OPM-2 (*upper panels*) or MM1.S (*lower panels*) in  
201 the presence or absence of CAFs.

202

203 **Supplemental Figure S5 | Bone marrow MSCs derived from healthy donor do not**  
204 **inhibit BCMA-CART proliferation.** BCMA-CART cells were co-cultured with lethally  
205 irradiated BCMA<sup>+</sup>SLAMF7<sup>+</sup>MM1.S (*left*) or BCMA<sup>+</sup>SLAMF7<sup>+</sup>OPM-2 (*right*) in the  
206 presence or absence of MSCs for 5 days. Absolute number of CD3<sup>+</sup> T cells were  
207 counted via flow cytometer (mean and SEM, t-test; n=6, 2 replicates).

208

209 **Supplemental Figure S6 | Actual values of cytokines from the multiplex assay.**  
210 Cytokines were analyzed by multiplex using supernatant from the co-culture of BCMA-  
211 CART and irradiated MM1.S with or without BM-CAFs (mean and SEM, \*p<0.05,  
212 \*\*p<0.01, \*\*\*\*p<0.0001, Student's t-test; n=3, 2 replicates).

213

214 **Supplemental Figure S7 | Inhibitory cytokines and growth factors were**

215 **increased, and effector cytokines were decreased in the presence of BM-CAFs.**  
216 BCMA-CART-cells were co-cultured with irradiated OPM-2 (A) or ALMC-2 (B) for 3  
217 days and supernatants were analyzed via multiplex. Bar graphs represent the raw  
218 values of cytokines (n.s. not significant, \*p<0.05, \*\*p<0.01, \*\*\*p<0.005, unpaired, two-  
219 sided, Student's t-test; n=3 experiments, 2 replicates).

220

221 **Supplemental Figure S8 | TGF- $\beta$  depletion does not overcome BM-CAF induced**  
222 **impairment of BCMA CART cytotoxicity.** BCMA-CART were co-cultured with  
223 MM1.S and BM-CAFs in the presence or absence of anti TGF- $\beta$  antibody. At 24 hours,  
224 cytotoxicity was assessed by luminescence relative to controls (\*\*p<0.001, two-way  
225 ANOVA; n=3, 2 replicates).

226

227 **Supplemental Figure S9 | Flow cytometric gating for assessment of inhibitory**  
228 **receptor-ligand expression.** BCMA-CART were co-cultured with lethally irradiated  
229 MM1.S and BM-CAFs. Cells were gated on FSC/SCC followed by singlet and live cell  
230 discrimination. CD3, CD38, CD45, and FSP-1 were used to distinguish CAFs from  
231 CART-cells. The surface PD-L1 or PD-L2 expression on BM-CAFs were assessed by  
232 flow cytometry. Isotype controls are shown as gray peaks.

233

234 **Supplemental Figure S10 | CAF inhibition of BCMA-CART-cell proliferation**  
235 **cannot be reversed by blocking PD-1/PD-L1 axis and/or TGF- $\beta$  neutralization.**  
236 BCMA-CART cells were co-cultured with lethally irradiated OPM-2 (A) or MM1.S (B)  
237 in the presence or absence of CAFs for 5 days. PD-L1 blocking antibody (20  $\mu$ g/mL)

238 and/or TGF- $\beta$  neutralizing antibody (1  $\mu$ g/mL) were also added to some conditions.  
239 Absolute number of CD3<sup>+</sup> T cells were assessed by flow cytometry on day 5 (mean  
240 and SEM, \*p<0.05, \*\*p<0.001, t-test; n=3, 2 replicates).

241

242 **Supplemental Figure S11 | Flow cytometry gating for BM-CAFs and CD45**  
243 **negative fraction derived from bone marrow of patients with multiple myeloma.**

244 **A**, Gating of BM-CAFs samples from patients with MM. The bone marrow was first  
245 isolated with CD138<sup>+</sup> microbeads. Then, CD138<sup>-</sup> fraction was cultured for two weeks  
246 and CAFs were isolated with anti-fibroblasts microbeads. BM-CAFs were defined as  
247 the live, CD45<sup>-</sup>CD38<sup>-</sup>FSP-1<sup>+</sup> fraction. **B**, Representative flow plots of BM-CAFs.  
248 Isotype control of IgG1-APC and IgG1-PE were used for left flow plots. SLAMF7-APC  
249 and FAP-PE were used for right flow plots.

250

251 **Supplemental Figure S12 | Flow cytometric analysis for BM-MSCs and qPCR**  
252 **analysis of BM-MSCs and BM-CAFs. A**, Flow cytometric analysis for BM-MSCs

253 derived from healthy donor. MSCs were defined as CD38<sup>-</sup>, CD45<sup>-</sup>, and FSP<sup>+</sup> cells.  
254 Grey peaks are fluorescence minus one (FMO) controls. Purple peaks are the stained  
255 samples. Representative histograms are shown; n=3. **B**, qPCR analysis for BM-MSC  
256 derived from healthy donors and BM-CAFs from MM patients (\*\* p<0.01, \*\*\*\* p<0.0001,  
257 Student's t-test; n=3, 3 replicates).

258

259 **Supplemental Figure S13 | Flow cytometric analysis of BCMA, SLAMF7, and FAP**  
260 **expression on OPM-2, MM1.S, and ALMC-2 cells.** Grey peaks represent the isotype

261 controls.

262

263 **Supplemental Figure S14| Constructs of the BCMA-, SLAMF7-, and FAP-CAR**  
264 **vector, and surface CAR expression on human CD3 T-cells. A,** Schematic  
265 representation of the BCMA-, SLAMF7-, and FAP-CAR constructs. BCMA-CAR  
266 consisted of anti-BCMA single chain variable fragment (scFv) linked to CD3 zeta and  
267 a 4-1BB costimulatory domain. H, hinge; TM, transmembrane. SLAMF7-CAR  
268 consisted of anti-SLAMF7 scFv linked to CD3 zeta and a CD28 costimulatory domain.  
269 FAP-CAR consisted of anti-FAP scFv linked to CD3 zeta and a 4-1BB costimulatory  
270 domain. **B,** Representative flow plots of UTDs, BCMA-, SLAMF7-, and FAP-CART.  
271 Goat anti-mouse F(ab')<sub>2</sub> antibody (GAM) was used with live/dead aqua to detect CAR  
272 expression on CART-cells. Cells were gated on FSC/SSC followed by singlet  
273 discrimination and live cells. Negative gates for CAR expression were set based on  
274 untransduced (UTD) T cells.

275

276 **Supplemental Figure S15 | Representative flow plots of FAP-CART**  
277 **degranulation assay.** FAP-CART stimulated with FAP<sup>+</sup>WI-38 or FAP-JeKo-1 cells.  
278 CD3 was used to distinguish CART-cells from target cells.

279

280 **Supplemental Figure S16 | Representative flow plots of SLAMF7-CART-cell**  
281 **degranulation assay.** SLAMF7-CART-cells stimulated with SLAMF7<sup>+</sup>MM1.S or  
282 SLAMF7-Jurkat cells. CD3 was used to distinguish CART-cells from target cells.

283

284 **Supplemental Figure S17 | SLAMF7- or FAP-CART cytotoxicity assay against**  
285 **BM-CAFs.** SLAMF7- or FAP-CART were co-cultured with BM-CAFs at 1:1 ratio. At 24  
286 hours, cytotoxicity was assessed relative to controls. CD105 and CD3 were used to  
287 differentiate CAF and T cells (mean and SEM, \*\* p<0.01, \*\*\* p<0.001, one-way  
288 ANOVA; n=3, 2 replicates).

289

290 **Supplemental Figure S18 | SLAMF7 or FAP-CART inhibit CAF growth *in vivo*.** **A,**  
291 Experimental schema. Four weeks after the injection of  $1 \times 10^6$  luciferase positive OPM-  
292 2 and  $1 \times 10^6$  BM-CAFs, mice were randomized into two groups: 1) SLAMF7-CART or  
293 2) FAP-CART. **B,** Tumor burden was assessed by BLI curve (mean and SEM, two-  
294 way ANOVA; n=3). **C,** Mice were euthanized when they reached an endpoint due to  
295 the high tumor load. Bone marrow was harvested and immunohistochemical staining  
296 was performed (H&E magnification 10, CD138 magnification 10, and FSP-1  
297 magnification 20).

298

299 **Supplemental Figure S19 | BCMA-, dual BCMA-SLAMF7-, or BCMA-FAP-CART**  
300 **degranulation and intracytoplasmic cytokine assay.** CART were co-cultured with  
301 OPM-2 and BM-CAFs for 4 hours and stained for CD107a and intracytoplasmic  
302 cytokines (mean and SEM, \*\*\*\*p<0.0001, \*\*\*p<0.001, \*\*p<0.01, one-way ANOVA; n=3,  
303 2 replicates).

304

305 **Supplemental Figure S20 | Cytokine and chemokine analysis of BCMA- or dual**  
306 **CART in the presence of BM-CAFs.** **A and B,** BCMA-, dual BCMA-SLAMF7- or

307 BCMA-FAP-CART were co-cultured with irradiated MM1.S (A) or OPM-2 (B) for 3 days  
308 in the presence of BM-CAFs and supernatant were analyzed for cytokines using  
309 multiplex (mean and SEM\* $p < 0.05$ , \*\* $p < 0.005$ , \*\*\* $p < 0.0005$ , \*\*\*\* $p < 0.0001$ , one-way  
310 ANOVA;  $n=2$ , 2 replicates).

311

312 **Supplemental Figure S21 | Anti-tumor efficacy of BCMA- and dual BCMA-**  
313 **SLAMF7-CART against OPM-2 and MM1.S cells *in vitro* and *in vivo*. A and B,**  
314 **BCMA or BCMA-CS1 CART cells equally lysed OPM-2 cells (A) or MM1.S cells (B)**  
315 **within 24 hours (two-way ANOVA;  $n=3$ , 2 replicates). C and D, CART CD107a**  
316 **degranulation assay upon stimulation of OPM-2 (C) or MM1.S (D) cells (mean and**  
317 **SEM, \*  $p < 0.05$ , \*\*  $p < 0.01$ , \*\*\*  $p < 0.001$ , \*\*\*\*  $p < 0.0001$ , one-way ANOVA),  $n=3$ , 2**  
318 **replicates. E-G, The head-to-head comparison of single BCMA-CART and dual**  
319 **BCMA-SLAMF7-CART in an OPM-2 xenograft mouse model. NSG mice were injected**  
320 **with  $1 \times 10^6$  of luciferase<sup>+</sup> OPM-2 cells on day -28. On day -1, tumor burden was**  
321 **assessed with bioluminescence imaging (BLI) and mice were randomized according**  
322 **to the tumor burden. On day 0, mice received  $1 \times 10^6$  of 1) UTD, 2) BCMA-CART, or 3)**  
323 **BCMA-SLAMF7-CART (mean and SEM, \*  $p < 0.05$  at day 13, two-way ANOVA;  $n=5$  per**  
324 **group). G, Kaplan-Meier curve of OPM-2 xenograft mouse model is shown [BCMA-**  
325 **CART vs. BCMA-SLAMF7-CART hazard ratio = 0.0630; 95% confidence interval (CI)**  
326 **= 0.005903-0.6722, \* $p=0.05$ ].**

327

328 **Supplemental Figure S22 | Dual BCMA-SLAMF7 targeting CART cells overcome**  
329 **BM-CAF-induced impairment of BCMA-CART killing. UTD, BCMA-CART, or**

330 BCMA-SLAMF7-CART-cells were co-cultured with luciferase positive OPM-2 cells at  
331 different E:T ratio, in the presence or absence of BM-CAFs (ratio of OPM-2: CAFs of  
332 1:0.1; at 0.6:1 ratio, mean and SEM, \*  $p < 0.05$ , \*\*  $p < 0.01$ , one-way ANOVA);  $n = 3$ , 2  
333 replicates.

334

335 **Supplemental Figure S23 | BCMA-SLAMF7- or BCMA-FAP-CART demonstrate a**  
336 **long-term durable response and improve overall survival in the MM-TME mouse**  
337 **model. A**, Experimental schema. Three weeks after the injection of  $1 \times 10^6$  luciferase<sup>+</sup>  
338 MM1.S and  $1 \times 10^6$  BM-CAFs, mice were randomized into four groups: 1) UTD, 2)  
339 BCMA-CART, 3) BCMA-SLAMF7-CART, or 4) BCMA-FAP-CART. Tumor burden was  
340 assessed by BLI (3 mice per group). **B** and **C**, Bioluminescent imaging of mice treated  
341 with UTD or CART (mean and SEM, \* $p < 0.05$ , two-way ANOVA at day 27). **D**, Kaplan-  
342 Meier survival curve is shown. [BCMA-CART vs. BCMA-SLAMF7-CART hazard ratio  
343 = 0.06518; 95% confidence interval (CI) = 0.006025 to 0.7051, \* $p = 0.02$ , BCMA-  
344 CART vs. BCMA-FAP-CART hazard ratio = 0.06518; 95% CI = 0.006025 to  
345 0.7051, \* $p = 0.02$ ].

346

347 **Supplemental Figure S24 | CART-cell expansion and the composition of CART**  
348 **at day 8 of the generation. A**, T cells were isolated from the healthy-donor-derived  
349 PBMCs. T cells were then stimulated with anti-CD3/CD28 beads at 1:3 (T cells:beads).  
350 CARs were lentivirally transduced on day 1 at an MOI of 3. T cells were counted on  
351 days 0, 3, 5, 6, and 8. Beads were removed from T cells on day 6. **B**, Representative  
352 flow plots of UTD, BCMA-, FAP-, SLAMF7-, BCMA-FAP-, and BCMA-SLAMF7-CART-



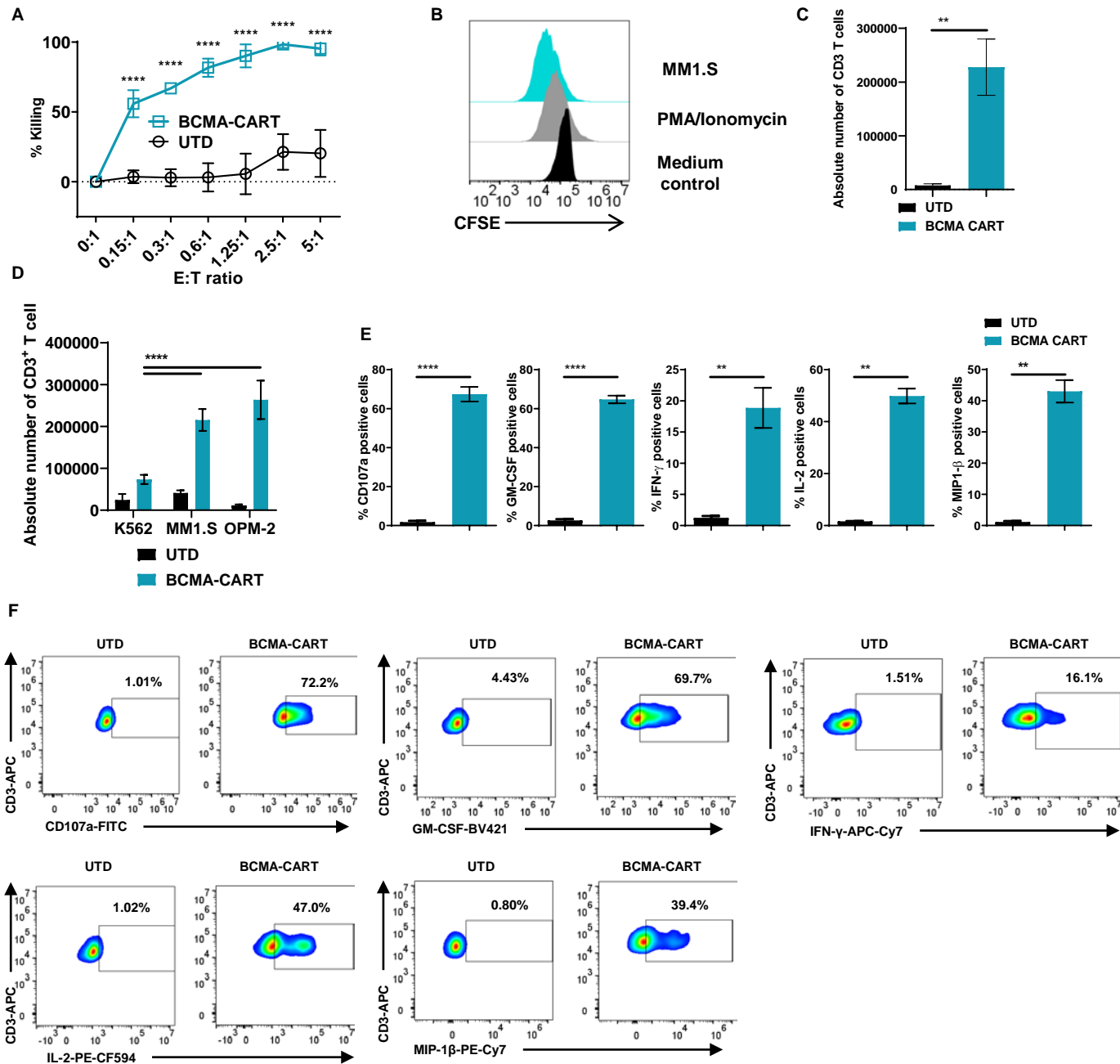
353 cells (n=3).

354 **Supplemental References:**

- 355 1. Sterner RM, Cox MJ, Sakemura R, Kenderian SS. Using CRISPR/Cas9 to  
356 Knock Out GM-CSF in CAR-T Cells. *Jove-Journal of Visualized Experiments*.  
357 2019(149).
- 358 2. Sterner RM, Sakemura R, Cox MJ, et al. GM-CSF inhibition reduces cytokine  
359 release syndrome and neuroinflammation but enhances CAR-T cell function in  
360 xenografts. *Blood*. 2019;133(7):697-709.
- 361 3. Carpenter RO, Evbuomwan MO, Pittaluga S, et al. B-cell maturation antigen  
362 is a promising target for adoptive T-cell therapy of multiple myeloma. *Clin Cancer Res*.  
363 2013;19(8):2048-2060.
- 364 4. van Rhee F, Szmania SM, Dillon M, et al. Combinatorial efficacy of anti-CS1  
365 monoclonal antibody elotuzumab (HuLuc63) and bortezomib against multiple  
366 myeloma. *Mol Cancer Ther*. 2009;8(9):2616-2624.
- 367 5. Tai YT, Dillon M, Song W, et al. Anti-CS1 humanized monoclonal antibody  
368 HuLuc63 inhibits myeloma cell adhesion and induces antibody-dependent cellular  
369 cytotoxicity in the bone marrow milieu. *Blood*. 2008;112(4):1329-1337.

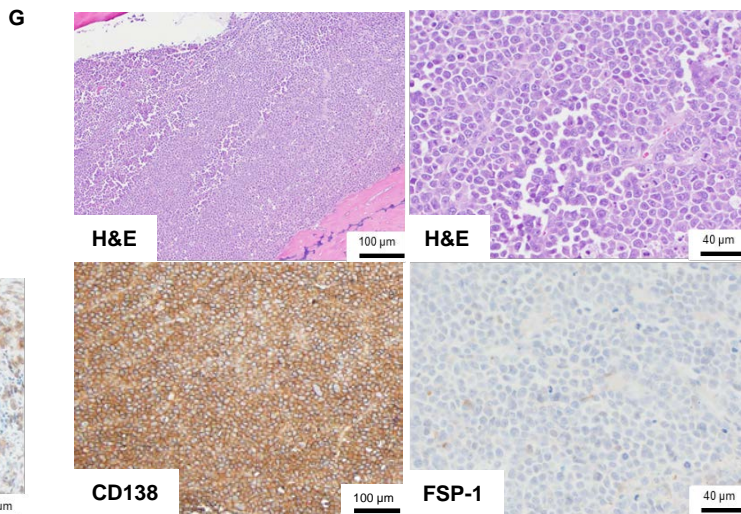
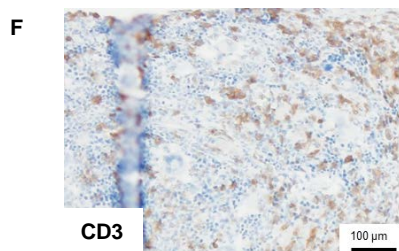
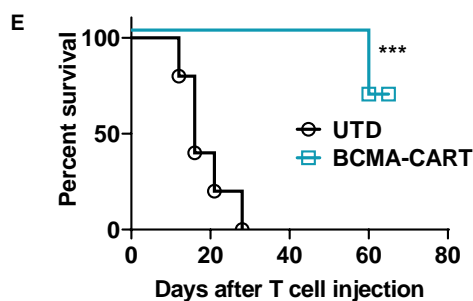
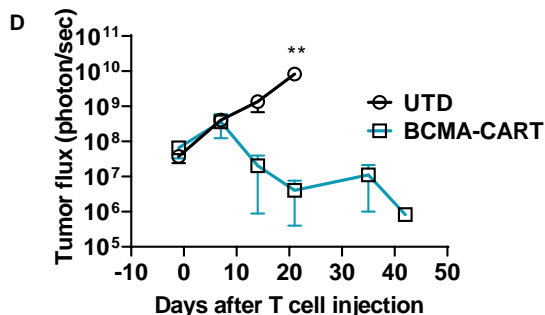
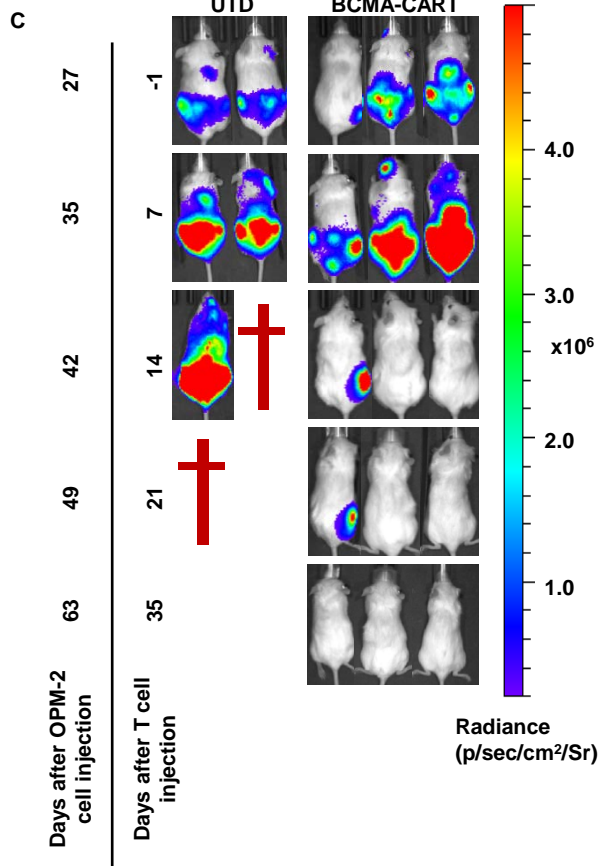
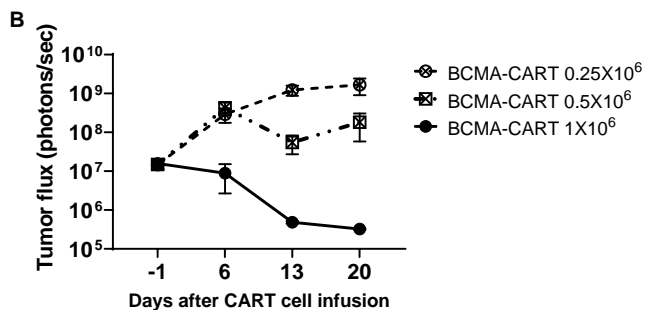
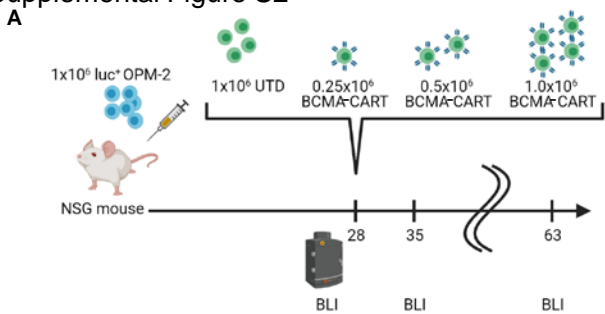
370

# Supplemental Figure S1



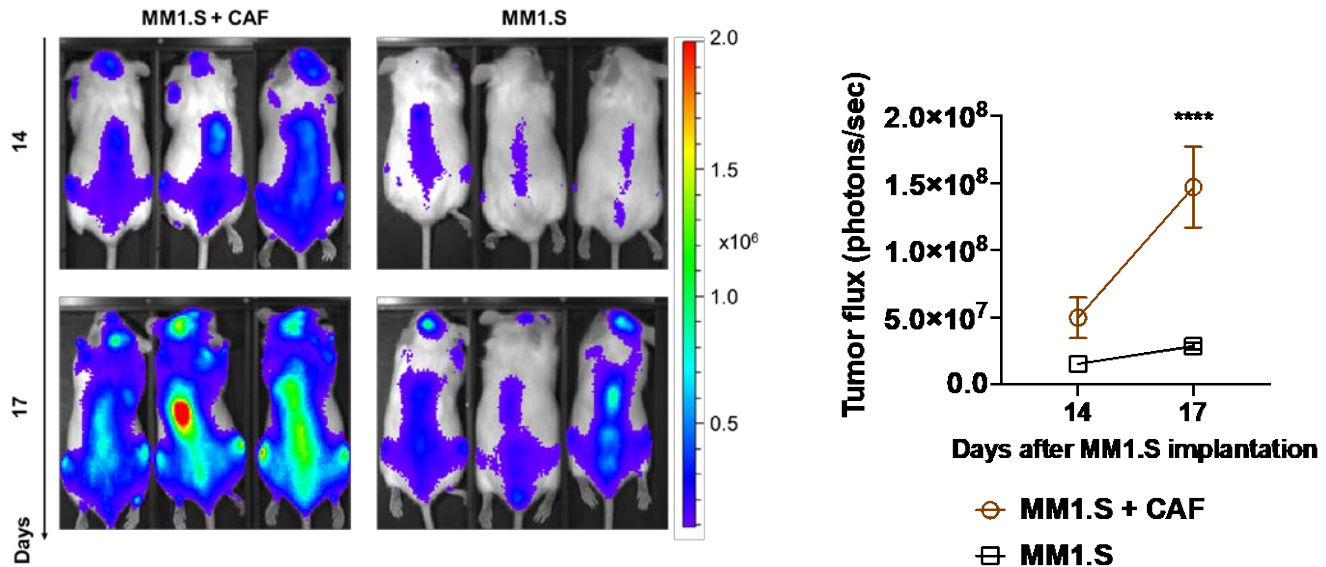
**Supplemental Figure S1 | Potent anti-tumor activity of BCMA-CART cells against BCMA expressing cells *in vitro*.** **A**, BCMA-CART-cells were co-cultured at different E:T ratios with luciferase<sup>+</sup> MM1.S. At 24 hours, cell killing was assessed by luminescence relative to controls (\*\*\*\*  $p < 0.0001$ , two-way ANOVA;  $n = 3$ , 2 replicates). **B**, CFSE-labeled BCMA-CART were co-cultured with lethally irradiated MM1.S for 5 days. Cells were then analyzed for CFSE dilution to detect cell proliferation, and absolute number of CART cells was counted by flow cytometry (5 ng/mL phorbol 12-myristate 13-acetate (PMA) and 0.1  $\mu$ g/mL ionomycin stimulation was used as a positive control;  $n = 3$ , 2 replicates). **C**, BCMA-CART-cells exhibited more antigen-specific proliferation compared to untransduced T cells (UTD). BCMA-CART or UTD derived from the same donor were co-cultured with lethally irradiated MM1.S for 5 days. Antigen-specific proliferation was measured by flow cytometry after 5 days using absolute counts with counting beads. **D**, BCMA-CART or UTD were co-cultured with lethally irradiated K562, MM1.S, or OPM-2 cells for 5 days. Absolute number of T cells were counted via flow cytometry (mean and SEM, \*\*\*\*  $p < 0.0001$ , one-way ANOVA;  $n = 3$ , 2 replicates). **E**, BCMA-CART cell degranulation and cytokine release assay. BCMA-CART degranulation assay and cytokine production. BCMA-CART or UTD were co-cultured with MM1.S for 4 hours. Medium was used as a negative control (mean and SEM, \*\*\*\*  $p < 0.0001$ , \*\*  $p < 0.005$ , one-way ANOVA;  $n = 3$ , 2 replicates). **F**, Representative flow plots of BCMA-CART or UTD CD107a degranulation and intracellular cytokine assays.

# Supplemental Figure S2

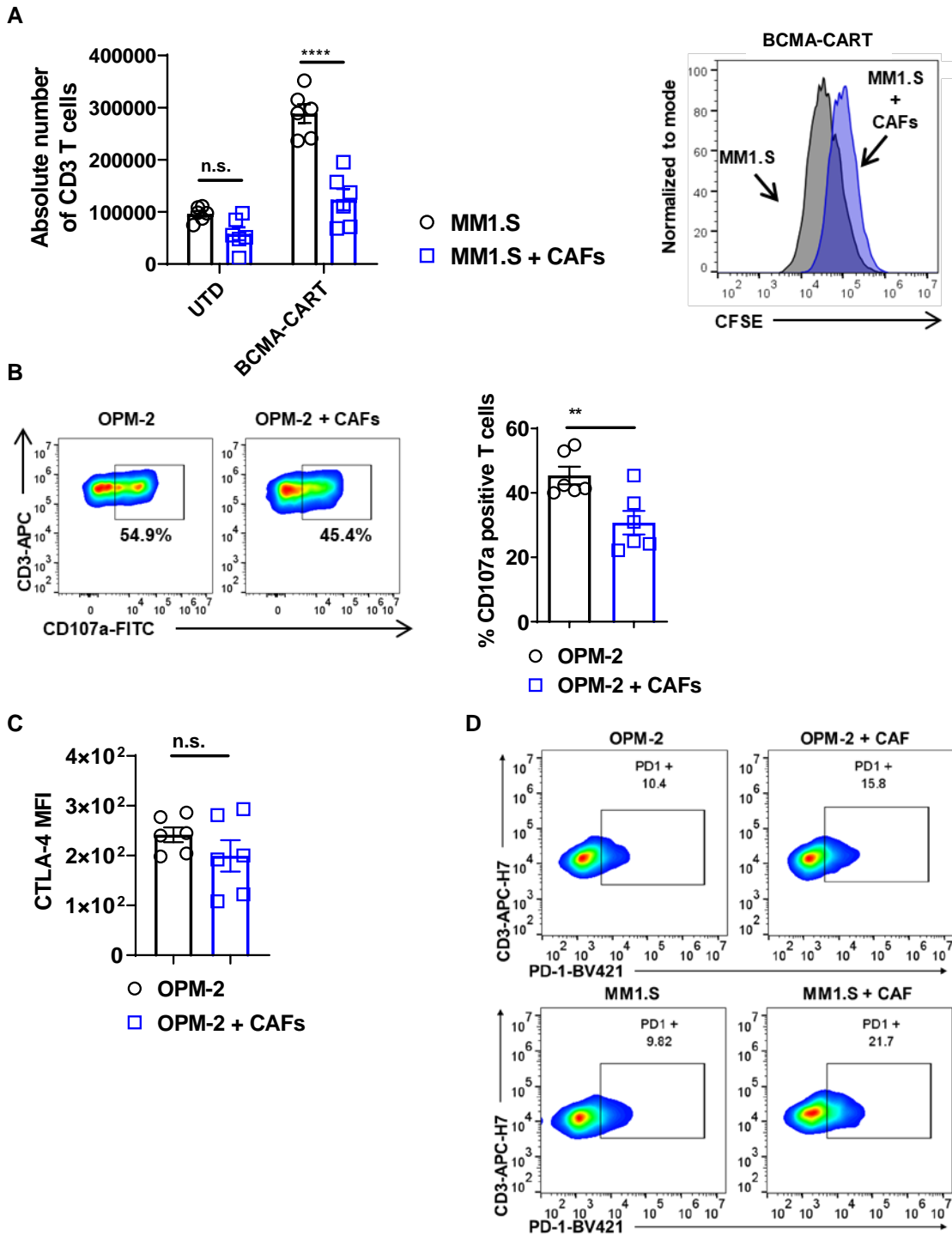


**Supplemental Figure S2 | Potent anti-tumor activity of BCMA-CART-cells against BCMA-expressing cells *in vivo*.** **A**, Experimental schema of BCMA-CART-cells in MM xenograft model. NSG mice were engrafted with luciferase<sup>+</sup>OPM-2 (1x10<sup>6</sup> cells/mouse, IV, 6 mice per group). On day 28, mice were randomized according to tumor burden, which was accessed by BLI, to receive 1x10<sup>6</sup> UTD, 1x10<sup>6</sup> BCMA-CART-cells, 0.5x10<sup>6</sup> BCMA-CART-cells, or 0.25x10<sup>6</sup> BCMA-CART-cells. **B**, BLI curve of *in vivo* BCMA-CART-cell dose-finding assay. **C-D**, Anti-myeloma activity of BCMA-CART-cells in OPM-2 xenograft mice, which was shown by bioluminescence imaging (mean and SEM, \*\*p=0.006 at day 21, unpaired, two-sided, Student's t-test). **E**, Kaplan-Meier survival curve is shown [hazard ratio = 0.03320; 95% confidence interval (CI) = 0.004605 to 0.2393, \*\*\*p=0.0007, log-rank test]. **F**, Immunohistochemical analysis of BM samples harvested from OPM-2 xenograft mice treated with BCMA-CART-cells (magnification 10). **G**, Immunohistochemical analysis of bone marrow from OPM-2 xenograft models, which were treated with UTD (H&E, upper left and right, magnification 10 and 40, respectively). CD138, lower left, magnification 10), and FSP-1 (lower right) staining revealed the absence of BM-CAFs in this model.

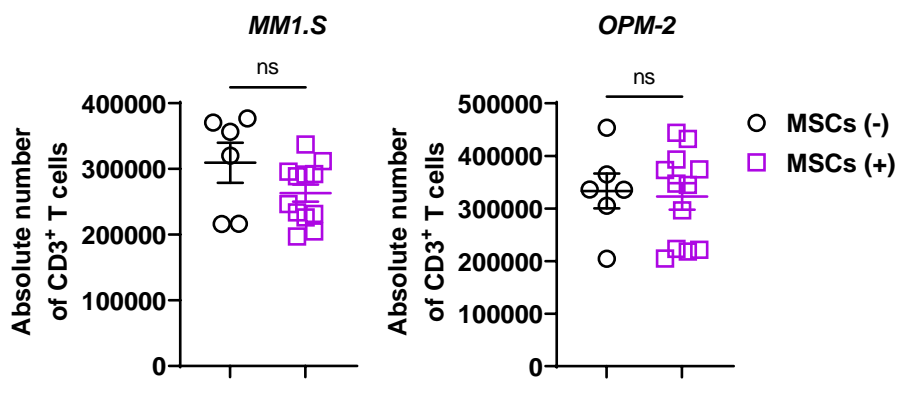
Supplemental Figure S3



**Supplemental Figure S3 | Bone marrow-derived cancer-associated fibroblasts (BM-CAFs) accelerate MM1.S cell growth *in vivo*.** NSG mice were intravenously injected with  $1 \times 10^6$  of luciferase<sup>+</sup> MM1.S cells or in combination with  $1 \times 10^6$  of BM-CAFs. Tumor growth was assessed with a bioluminescence imager (mean and SEM, \*\*\*\*  $p < 0.0001$ , two-way ANOVA;  $n = 3$ ).

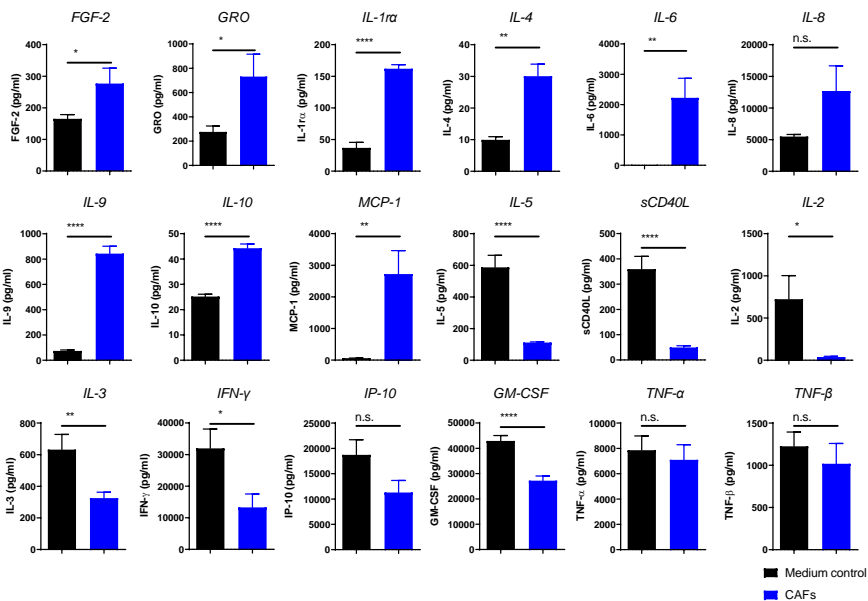


**Supplemental Figure S4 | BM-CAFs inhibit BCMA-CART effector functions.** **A**, CFSE-labeled BCMA-CART or UTD were co-cultured with lethally irradiated BCMA+SLAMF7+MM1.S and BM-CAFs for 5 days (mean and SEM, \*\*\*\* $p < 0.0001$ , two-way ANOVA;  $n = 3$ , 2 replicates). **B**, Antigen-specific BCMA-CART CD107a degranulation assay in the presence of BM-CAFs. OPM-2 cells were used as a stimulator (\*\* $p < 0.01$ , unpaired, two-sided, Student's t-test;  $n = 3$ , 2 replicates). **C**, CTLA-4 expression on BCMA-CART in the presence or absence of CAFs (Student's t-test;  $n = 3$ , 2 replicates). **D**, Representative flow plots of surface PD-1 expression on BCMA-CART cells when co-cultured with OPM-2 (*upper panels*) or MM1.S (*lower panels*) in the presence or absence of CAFs.



**Supplemental Figure S5 | Bone marrow MSCs derived from healthy donor do not inhibit BCMA-CART proliferation.** BCMA-CART cells were co-cultured with lethally irradiated BCMA+SLAMF7+MM1.S (*left*) or BCMA+SLAMF7+OPM-2 (*right*) in the presence or absence of MSCs for 5 days. Absolute number of CD3+ T cells were counted via flow cytometer (mean and SEM, t-test; n=6, 2 replicates).

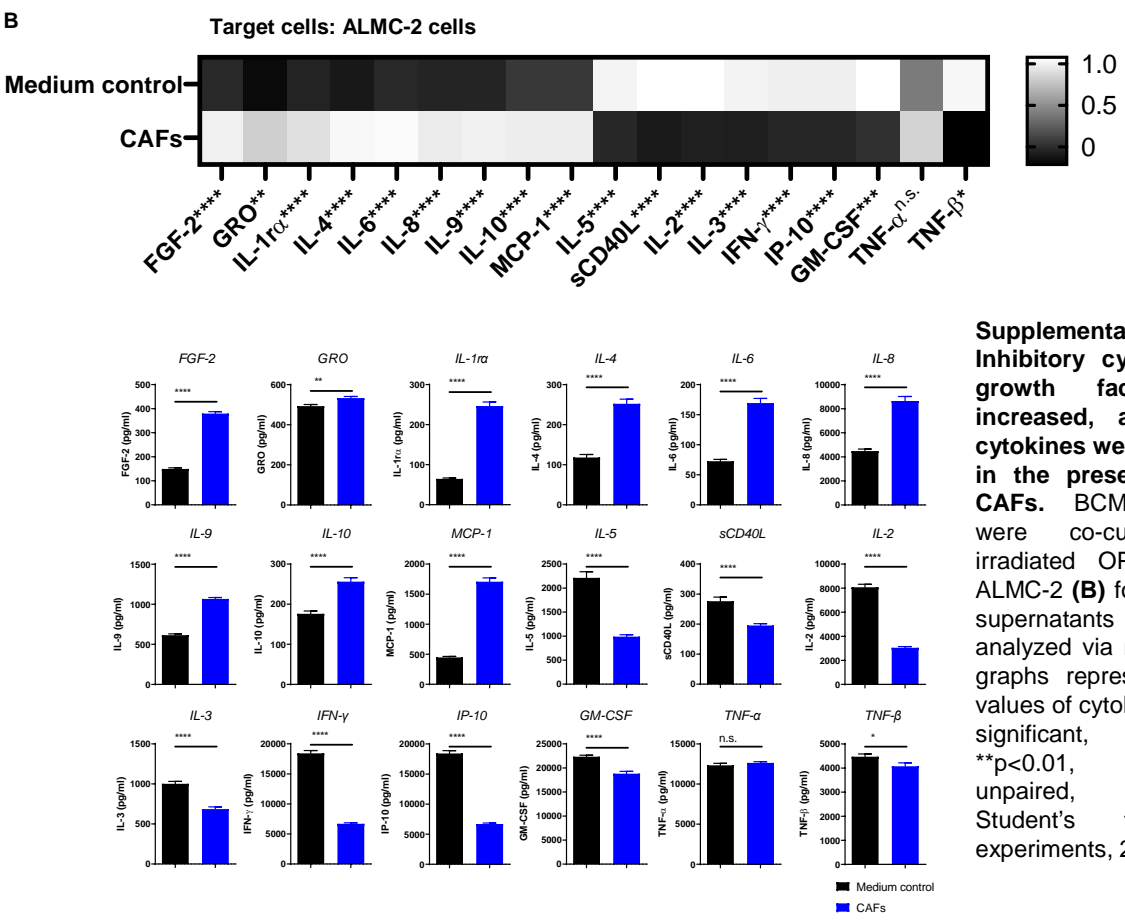
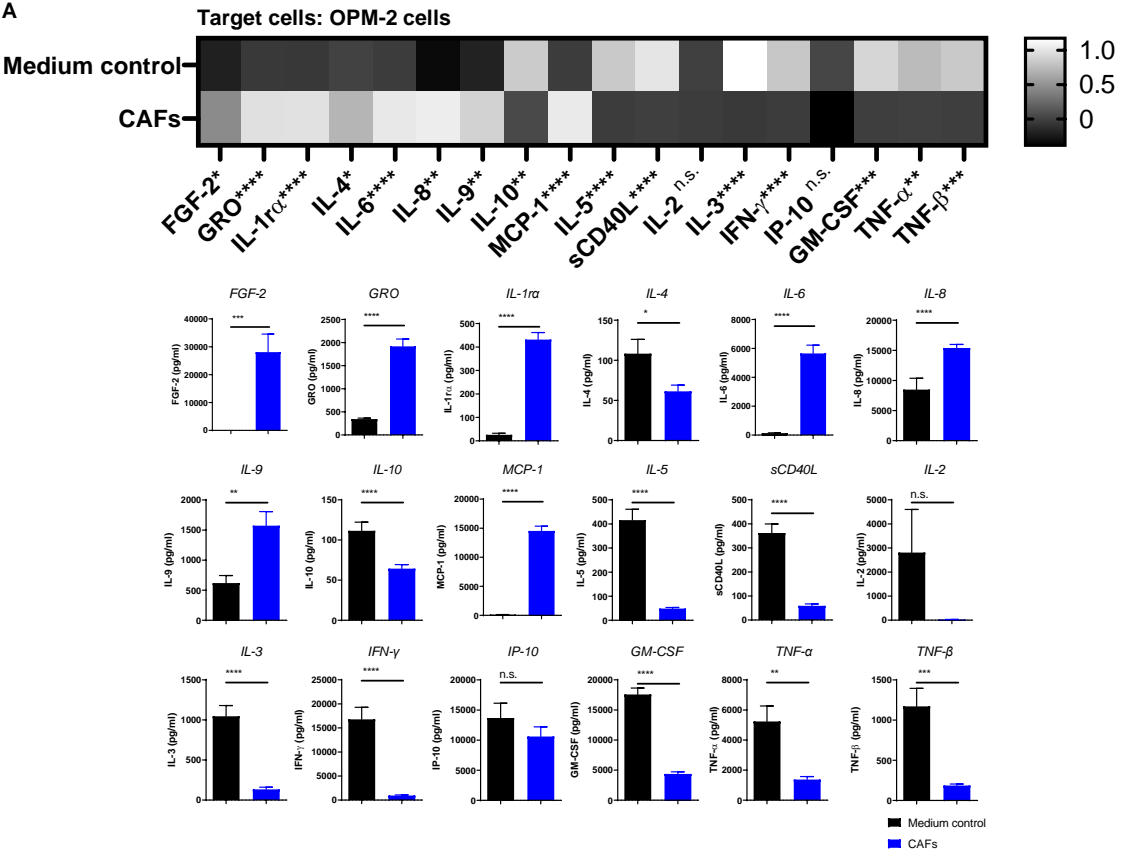
# Supplemental Figure S6



**Supplemental Figure S6 | Actual values of cytokines from the multiplex assay.** Cytokines were analyzed by multiplex using supernatant from the co-culture of BCMA-CART and irradiated MM1.S with or without BM-CAFs (mean and SEM, \* $p < 0.05$ , \*\* $p < 0.01$ , \*\*\* $p < 0.0001$ , Student's t-test;  $n = 3$ , 2 replicates).

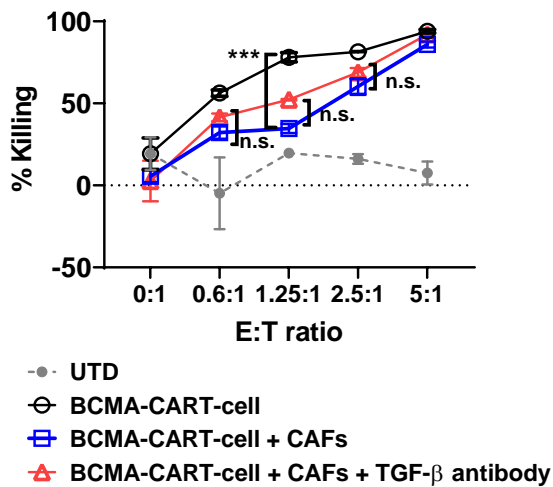


Supplemental Figure S7

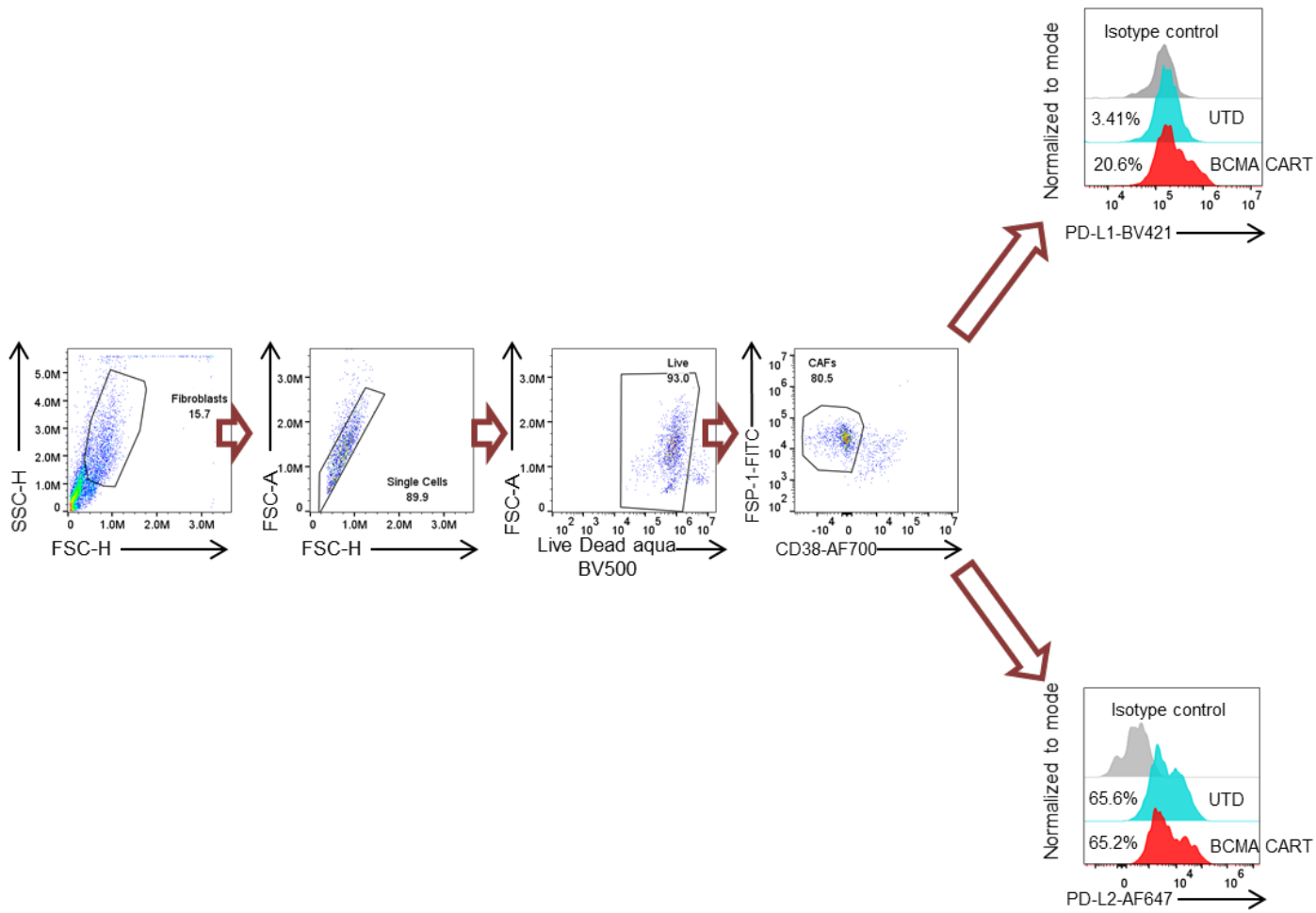


**Supplemental Figure S7 | Inhibitory cytokines and growth factors were increased, and effector cytokines were decreased in the presence of BM-CAFs.** BCMA-CART-cells were co-cultured with irradiated OPM-2 (A) or ALMC-2 (B) for 3 days and supernatants were analyzed via multiplex. Bar graphs represent the raw values of cytokines (n.s. not significant, \*p<0.05, \*\*p<0.01, \*\*\*p<0.005, unpaired, two-sided, Student's t-test; n=3 experiments, 2 replicates).

Supplemental Figure S8

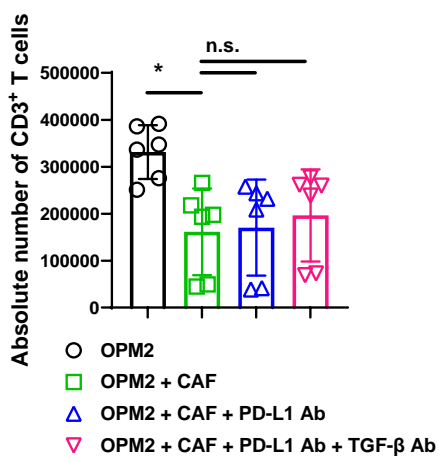


**Supplemental Figure S8 | TGF-β depletion does not overcome BM-CAF induced impairment of BCMA CART cytotoxicity.** BCMA-CART were co-cultured with MM1.S and BM-CAFs in the presence or absence of anti TGF-β antibody. At 24 hours, cytotoxicity was assessed by luminescence relative to controls (\*\*\*) p < 0.001, two-way ANOVA; n=3, 2 replicates).

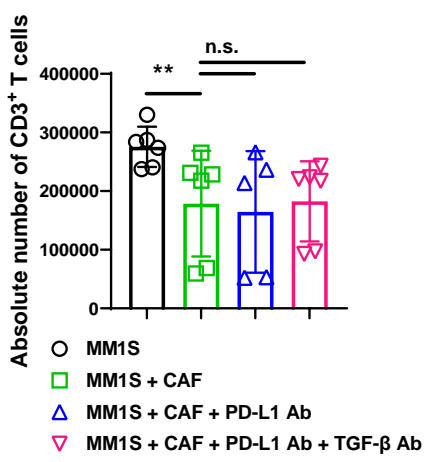


**Supplemental Figure S9 | Flow cytometric gating for assessment of inhibitory receptor-ligand expression.** BCMA-CART were co-cultured with lethally irradiated MM1.S and BM-CAFs. Cells were gated on FSC/SSC followed by singlet and live cell discrimination. CD3, CD38, CD45, and FSP-1 were used to distinguish CAFs from CART-cells. The surface PD-L1 or PD-L2 expression on BM-CAFs were assessed by flow cytometry. Isotype controls are shown as gray peaks.

A



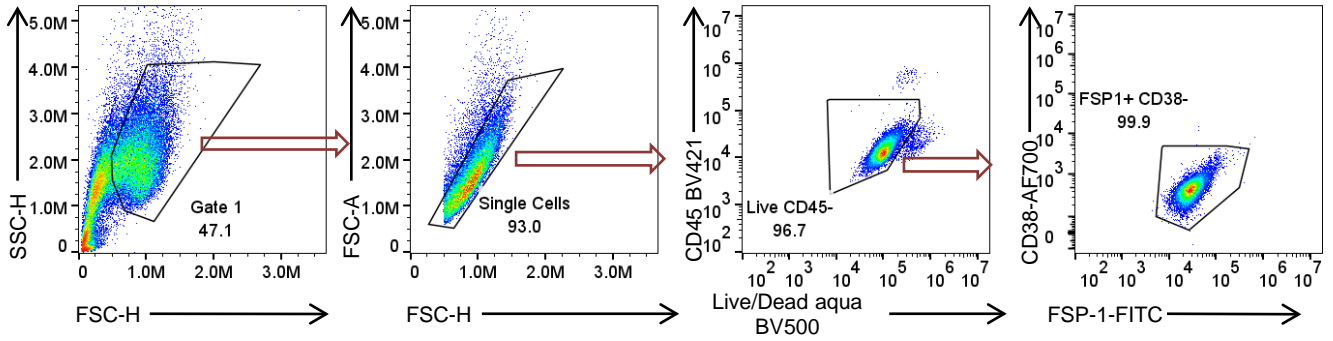
B



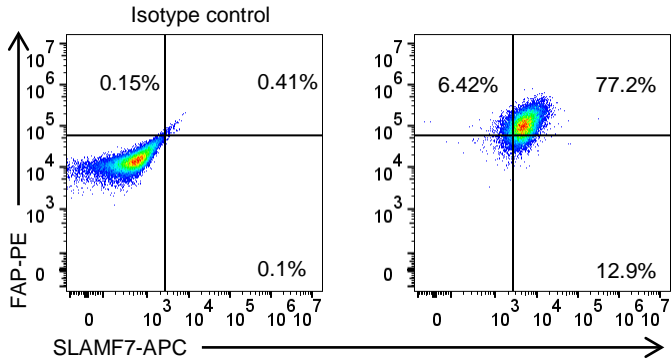
**Supplemental Figure S10 | CAF inhibition of BCMA-CART-cell proliferation cannot be reversed by blocking PD-1/PD-L1 axis and/or TGF-β neutralization.** BCMA-CART cells were co-cultured with lethally irradiated OPM-2 (A) or MM1.S (B) in the presence or absence of CAFs for 5 days. PD-L1 blocking antibody (20 μg/mL) and/or TGF-β neutralizing antibody (1 μg/mL) were also added to some conditions. Absolute number of CD3<sup>+</sup> T cells were assessed by flow cytometry on day 5 (mean and SEM, \*p<0.05, \*\*p<0.001, t-test; n=3, 2 replicates).

Supplemental Figure S11

**A**

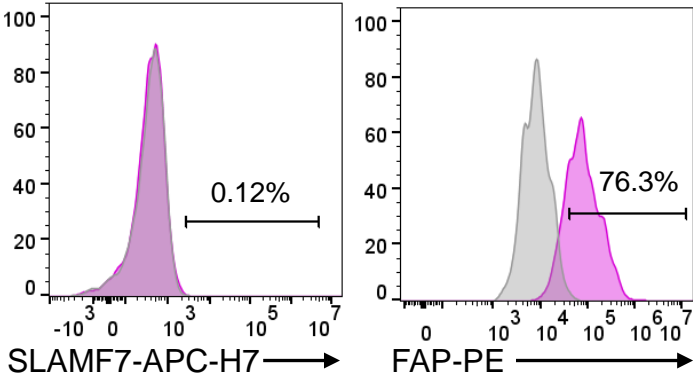


**B**

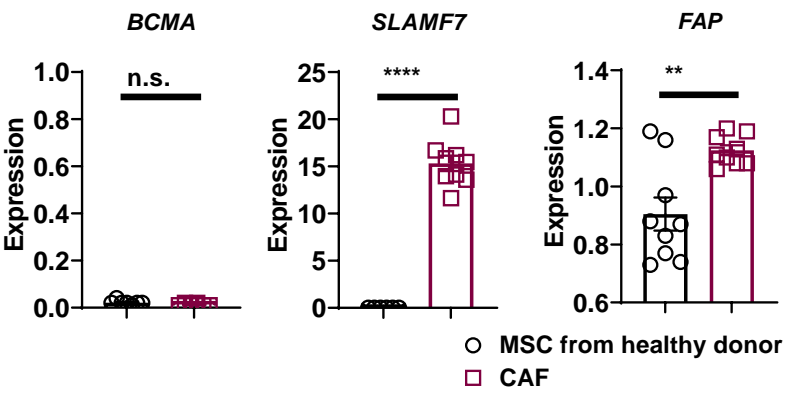


**Supplemental Figure S11 | Flow cytometry gating for BM-CAFs and CD45 negative fraction derived from bone marrow of patients with multiple myeloma. A,** Gating of BM-CAFs samples from patients with MM. The bone marrow was first isolated with CD138<sup>+</sup> microbeads. Then, CD138<sup>-</sup> fraction was cultured for two weeks and CAFs were isolated with anti-fibroblasts microbeads. BM-CAFs were defined as the live, CD45<sup>-</sup>CD38<sup>-</sup>FSP-1<sup>+</sup> fraction. **B,** Representative flow plots of BM-CAFs. Isotype control of IgG1-APC and IgG1-PE were used for left flow plots. SLAMF7-APC and FAP-PE were used for right flow plots.

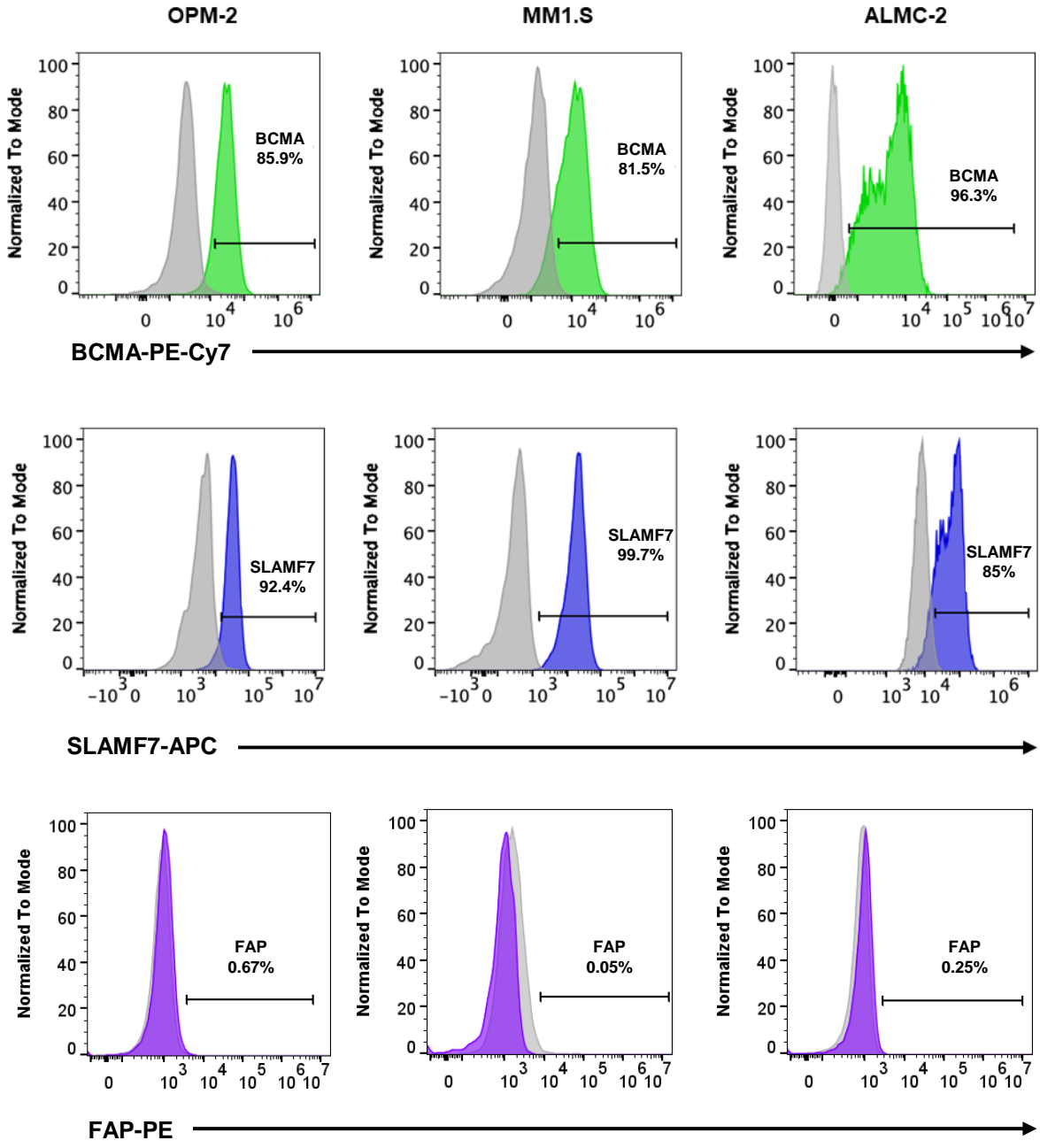
**A**



**B**

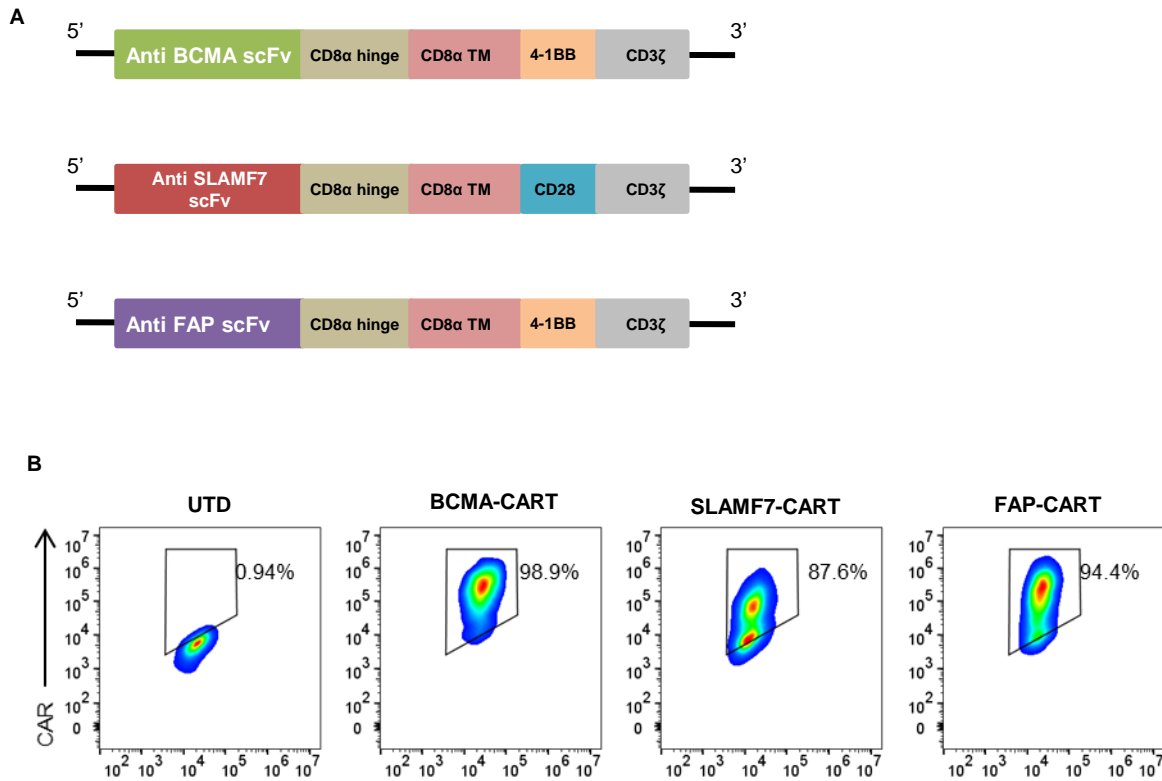


**Supplemental Figure S12 | Flow cytometric analysis for BM-MSCs and qPCR analysis of BM-MSCs and BM-CAFs. A,** Flow cytometric analysis for BM-MSCs derived from healthy donor. MSCs were defined as CD38<sup>-</sup>, CD45<sup>-</sup>, and FSP<sup>+</sup> cells. Grey peaks are fluorescence minus one (FMO) controls. Purple peaks are the stained samples. Representative histograms are shown; n=3. **B,** qPCR analysis for BM-MSC derived from healthy donors and BM-CAFs from MM patients (\*\* p<0.01, \*\*\*\* p<0.0001, Student's t-test; n=3, 3 replicates).



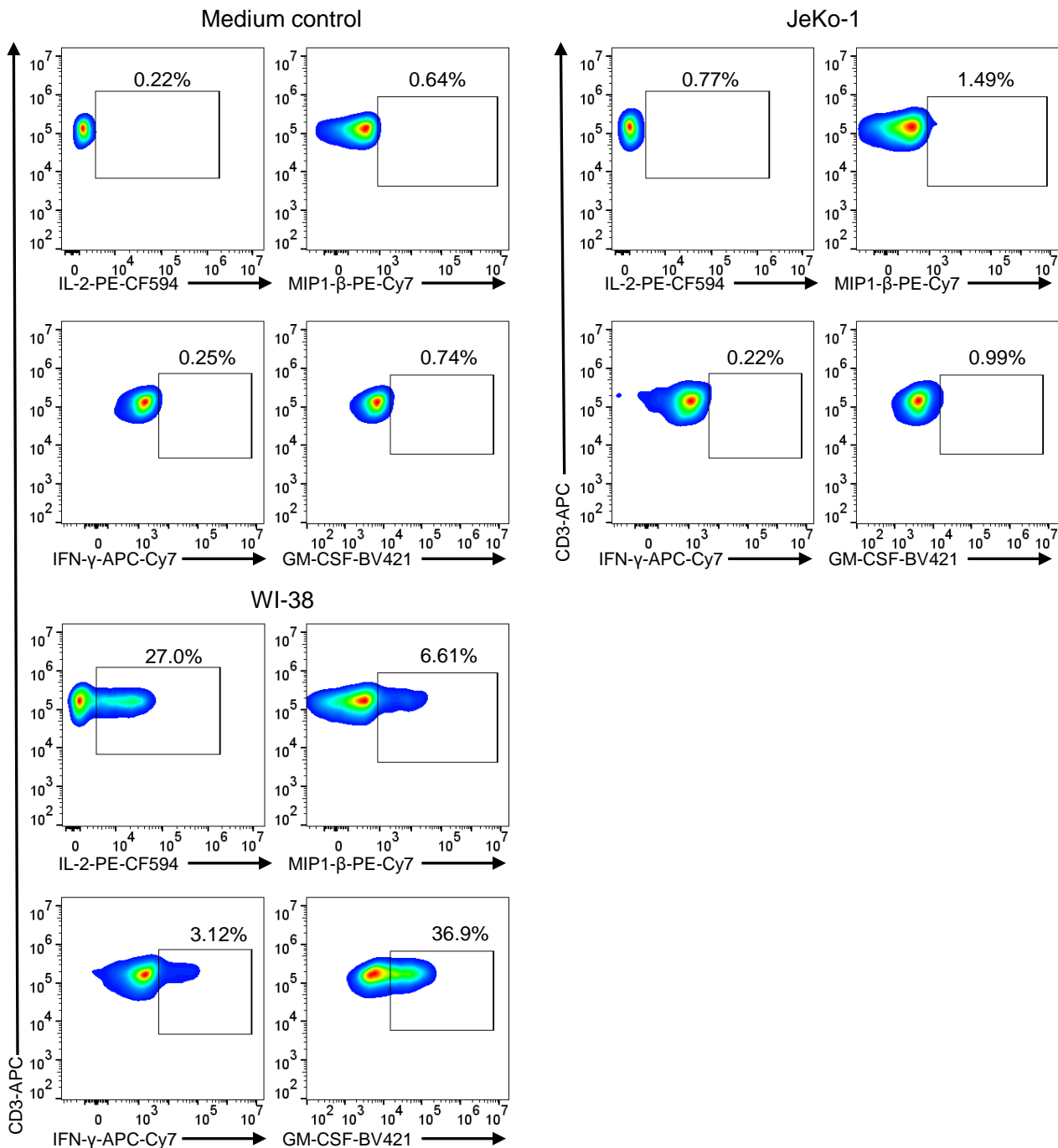
Supplemental Figure S13 | Flow cytometric analysis of BCMA, SLAMF7, and FAP expression on OPM-2, MM1.S, and ALMC-2 cells. Grey peaks represent the isotype controls.

## Supplemental Figure S14

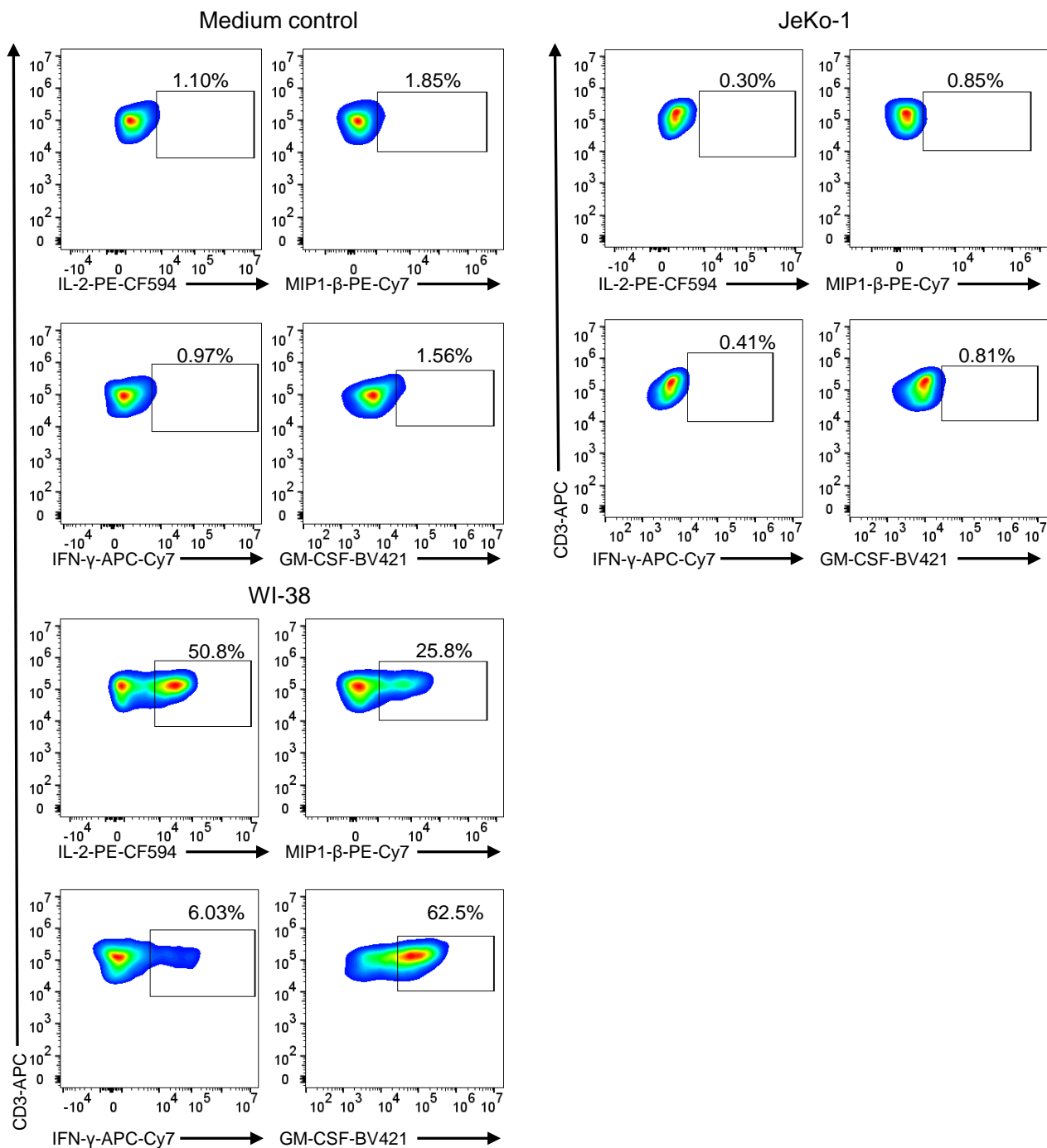


**Supplemental Figure S14| Constructs of the BCMA-, SLAMF7-, and FAP-CAR vector, and surface CAR expression on human CD3 T-cells. A**, Schematic representation of the BCMA-, SLAMF7-, and FAP-CAR constructs. BCMA-CAR consisted of anti-BCMA single chain variable fragment (scFv) linked to CD3 zeta and a 4-1BB costimulatory domain. H, hinge; TM, transmembrane. SLAMF7-CAR consisted of anti-SLAMF7 scFv linked to CD3 zeta and a CD28 costimulatory domain. FAP-CAR consisted of anti-FAP scFv linked to CD3 zeta and a 4-1BB costimulatory domain. **B**, Representative flow plots of UTDs, BCMA-, SLAMF7-, and FAP-CART. Goat anti-mouse F(ab')<sub>2</sub> antibody (GAM) was used with live/dead aqua to detect CAR expression on CART-cells. Cells were gated on FSC/SSC followed by singlet discrimination and live cells. Negative gates for CAR expression were set based on untransduced (UTD) T cells.

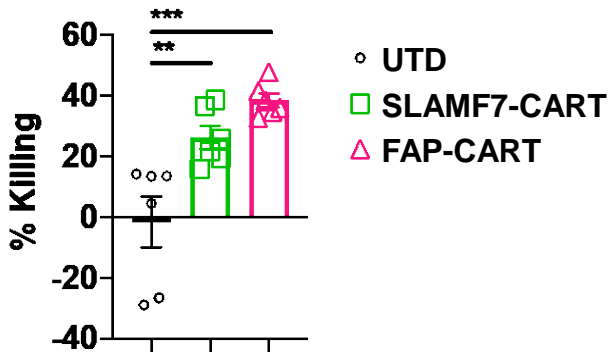
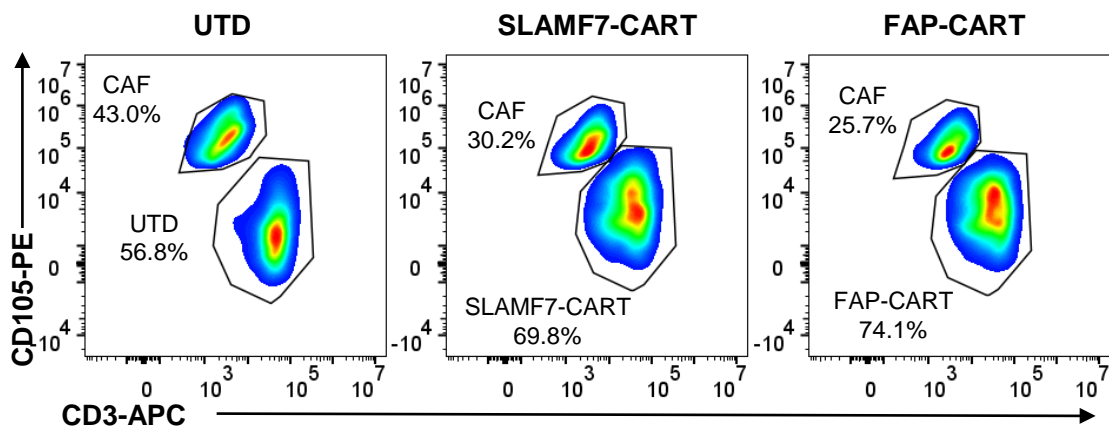




**Supplemental Figure S15 | Representative flow plots of FAP-CART degranulation assay.** FAP-CART stimulated with FAP<sup>+</sup>WI-38 or FAP<sup>+</sup>JeKo-1 cells. CD3 was used to distinguish CART-cells from target cells.

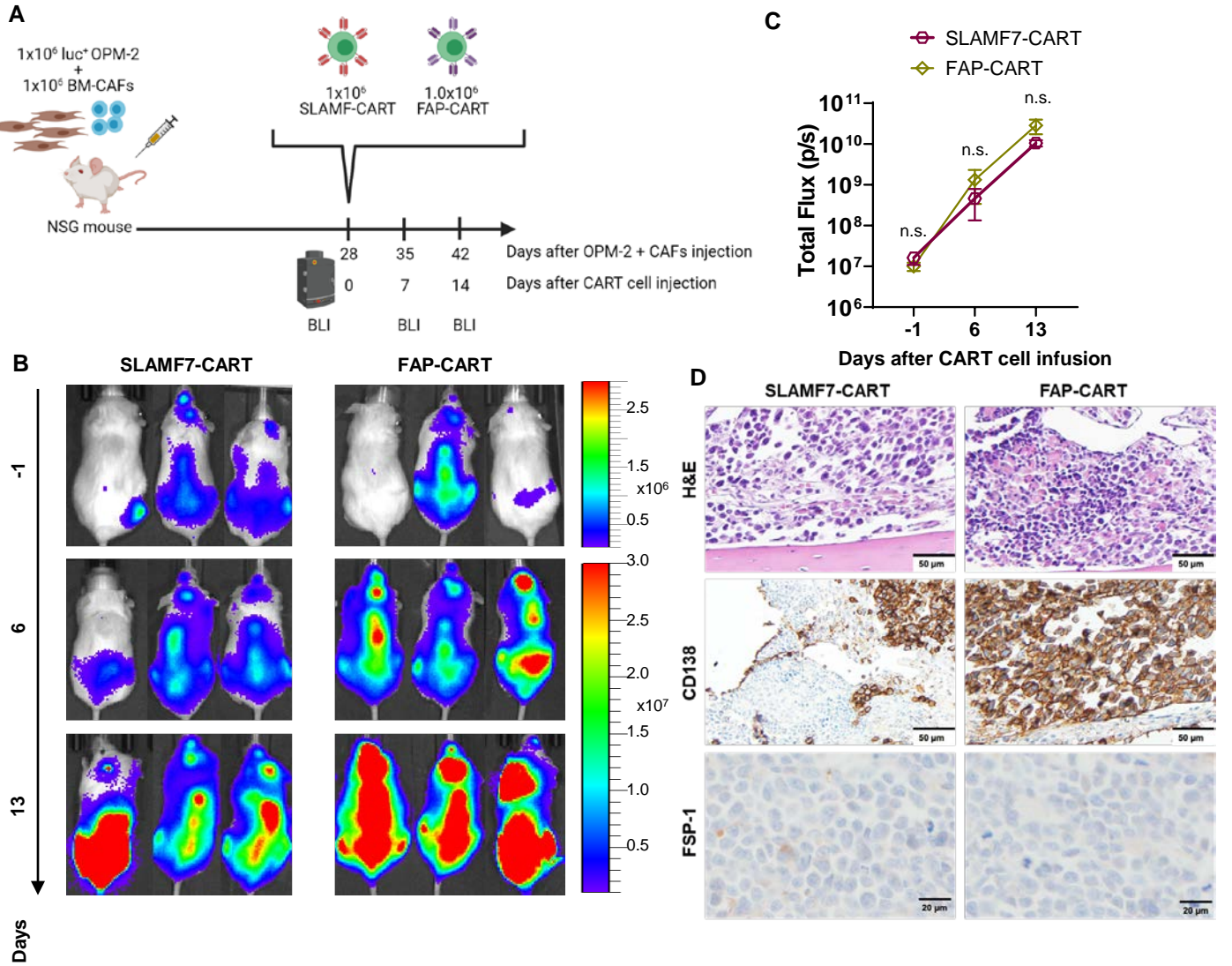


**Supplemental Figure S16 | Representative flow plots of SLAMF7-CART-cell degranulation assay.** SLAMF7-CART-cells stimulated with SLAMF7+MM1.S or SLAMF7-Jurkat cells. CD3 was used to distinguish CART-cells from target cells.

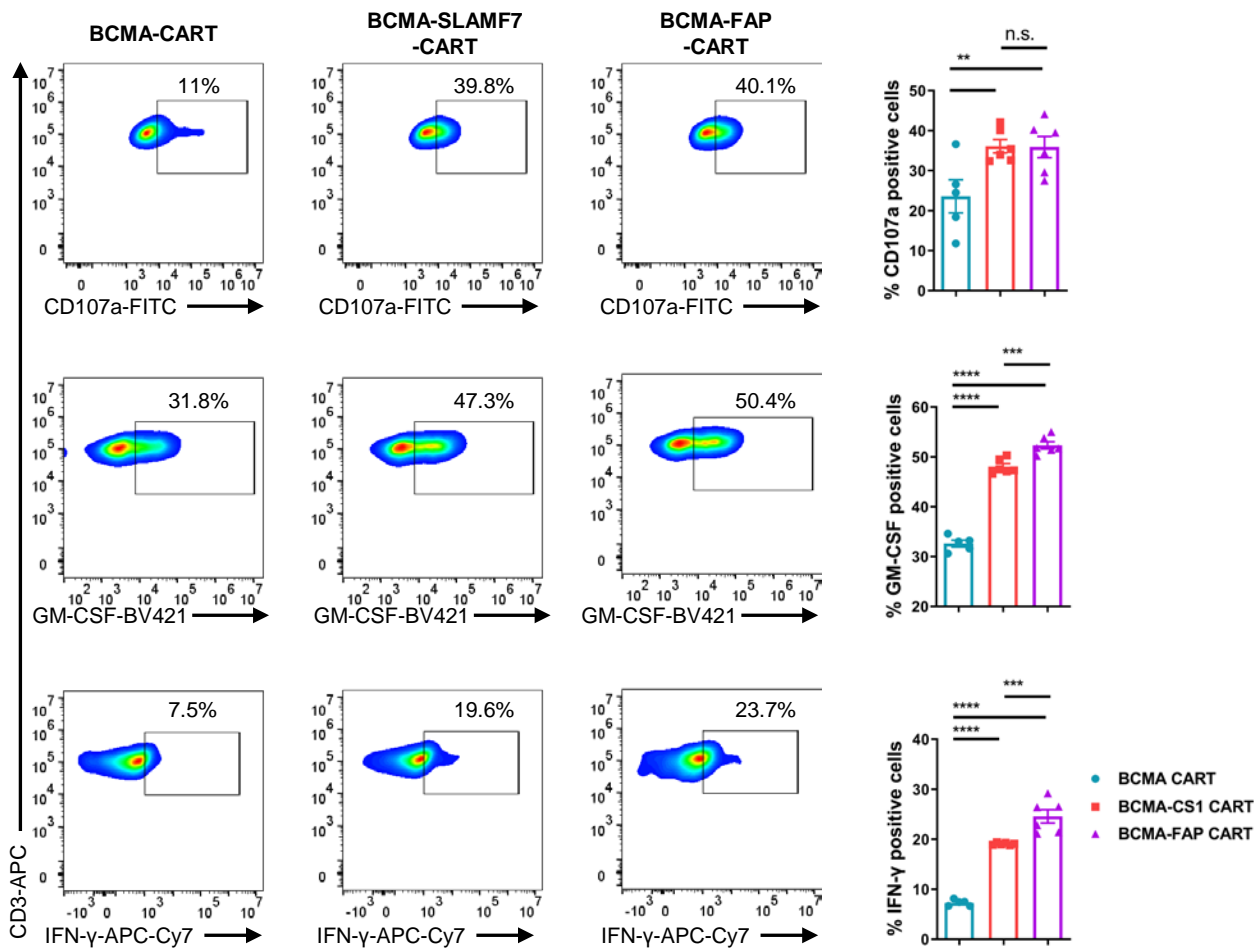


**Supplemental Figure S17 | SLAMF7- or FAP-CART cytotoxicity assay against BM-CAFs.** SLAMF7- or FAP-CART were co-cultured with BM-CAFs at 1:1 ratio. At 24 hours, cytotoxicity was assessed relative to controls. CD105 and CD3 were used to differentiate CAF and T cells (mean and SEM, \*\* p<0.01, \*\*\* p<0.001, one-way ANOVA; n=3, 2 replicates).

Supplemental Figure S18

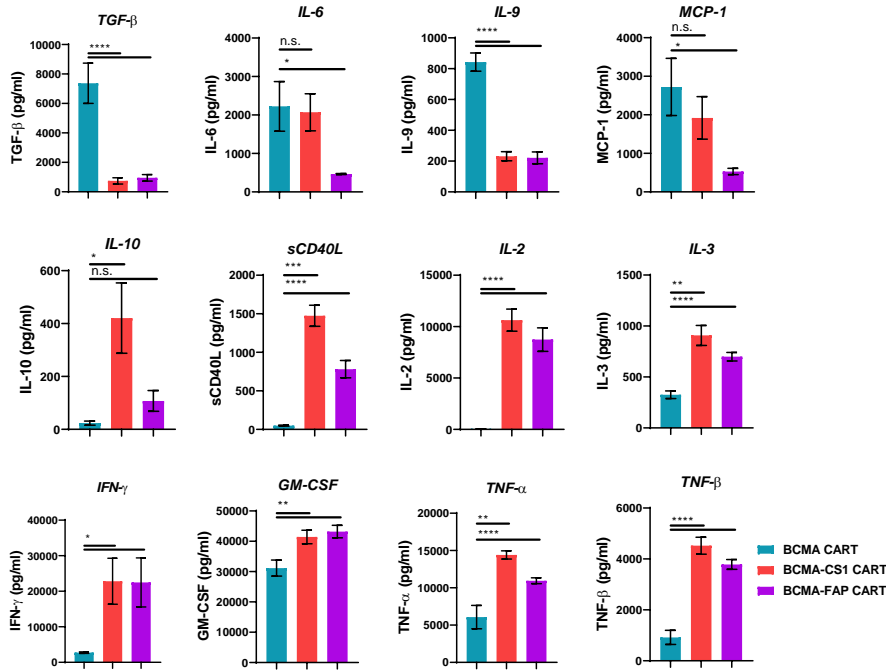


**Supplemental Figure S18 | SLAMF7 or FAP-CART inhibit CAF growth *in vivo*.** **A**, Experimental schema. Four weeks after the injection of 1x10<sup>6</sup> luciferase positive OPM-2 and 1x10<sup>6</sup> BM-CAFs, mice were randomized into two groups: 1) SLAMF7-CART or 2) FAP-CART. **B**, Tumor burden was assessed by BLI curve (mean and SEM, two-way ANOVA; n=3). **C**, Mice were euthanized when they reached an endpoint due to the high tumor load. Bone marrow was harvested and immunohistochemical staining was performed (H&E magnification 10, CD138 magnification 10, and FSP-1 magnification 20).

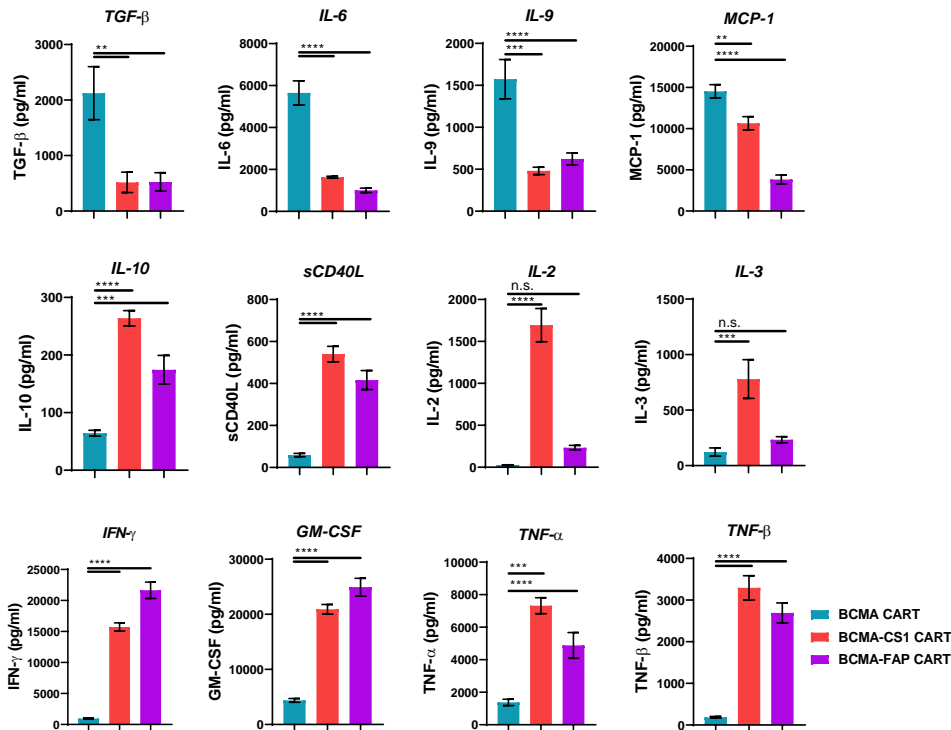


**Supplemental Figure S19 | BCMA-, dual BCMA-SLAMF7-, or BCMA-FAP-CART degranulation and intracytoplasmic cytokine assay.** CART were co-cultured with OPM-2 and BM-CAFs for 4 hours and stained for CD107a and intracytoplasmic cytokines (mean and SEM, \*\*\*\*p<0.0001, \*\*\*p<0.001, \*\*p<0.01, one-way ANOVA; n=3, 2 replicates).

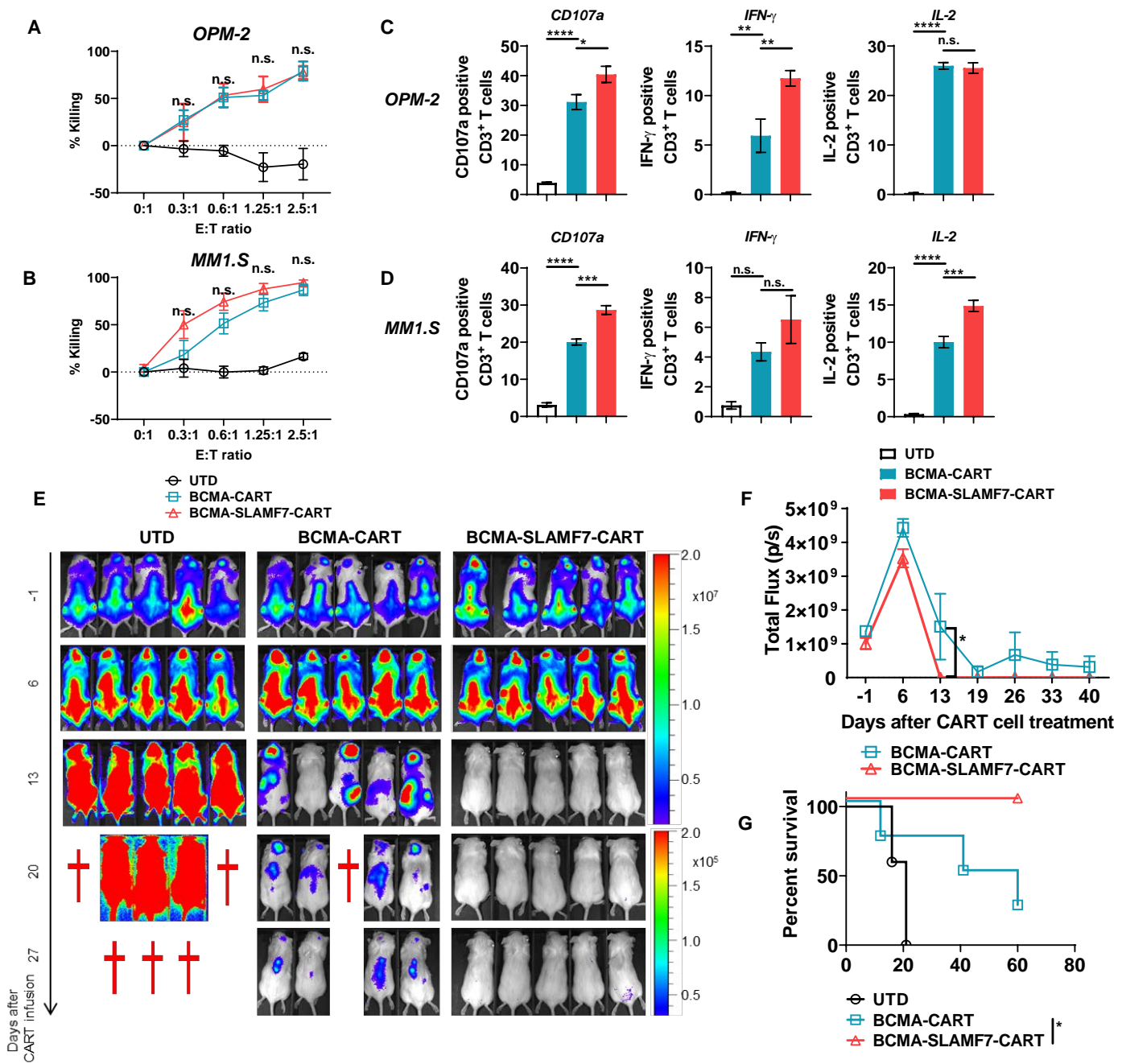
**A. Target cells: MM1.S cells**



**B. Target cells: OPM-2 cells**

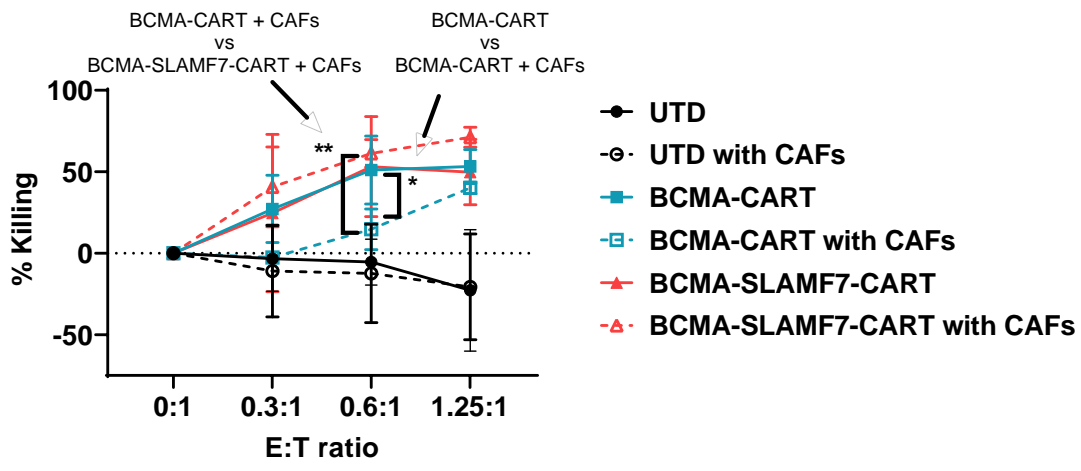


**Supplemental Figure S20 | Cytokine and chemokine analysis of BCMA- or dual CART in the presence of BM-CAFs. A and B,** BCMA-, dual BCMA-SLAMF7- or BCMA-FAP-CART were co-cultured with irradiated MM1.S (A) or OPM-2 (B) for 3 days in the presence of BM-CAFs and supernatant were analyzed for cytokines using multiplex (mean and SEM\* $p < 0.05$ , \*\* $p < 0.005$ , \*\*\* $p < 0.0005$ , \*\*\*\* $p < 0.0001$ , one-way ANOVA;  $n = 2$ , 2 replicates).



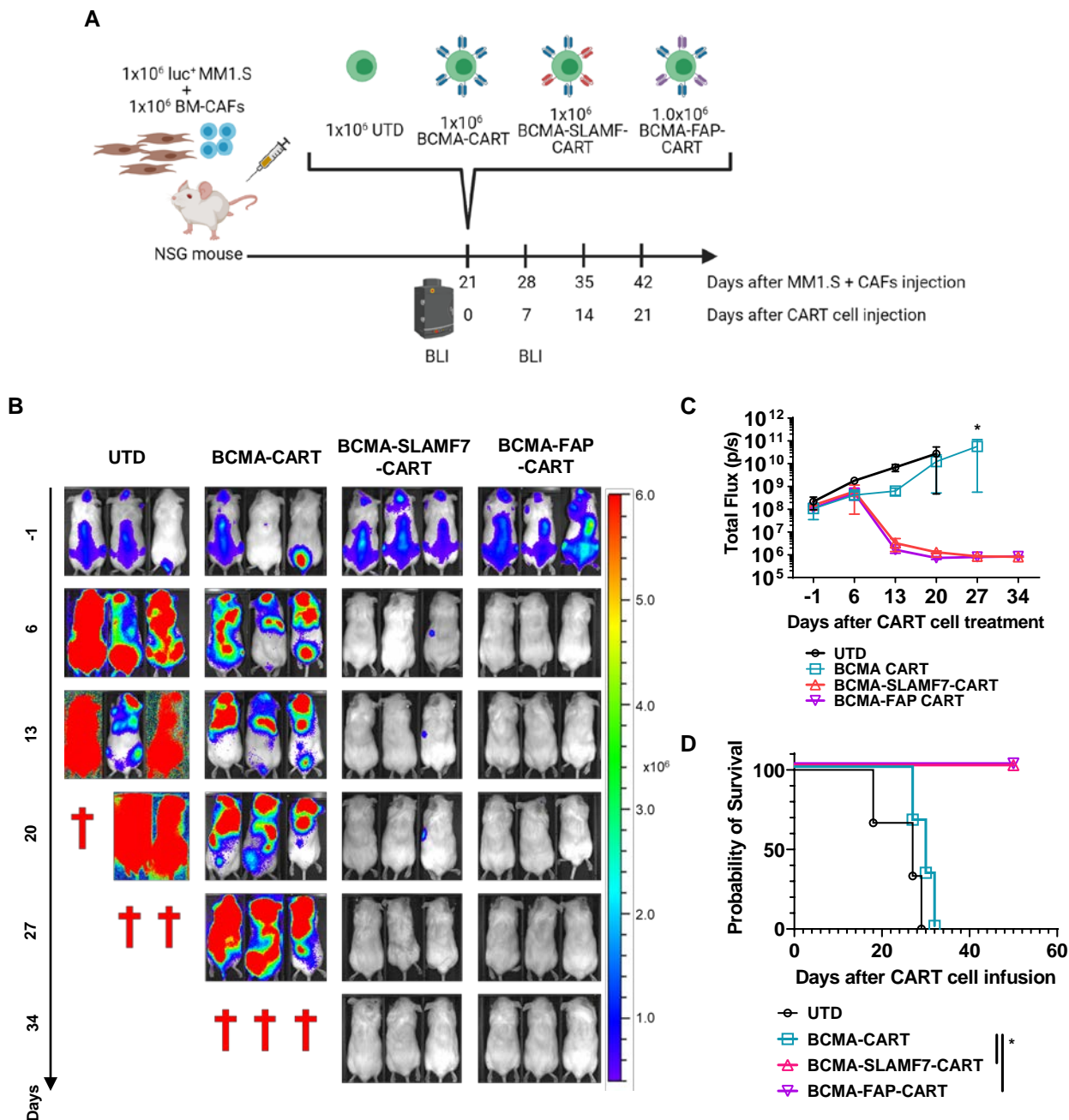
**Supplemental Figure S21 | Anti-tumor efficacy of BCMA- and dual BCMA-SLAMF7-CART against OPM-2 and MM1.S cells *in vitro* and *in vivo*.** **A** and **B**, BCMA or BCMA-CS1 CART cells equally lysed OPM-2 cells (**A**) or MM1.S cells (**B**) within 24 hours (two-way ANOVA; n=3, 2 replicates). **C** and **D**, CART CD107a degranulation assay upon stimulation of OPM-2 (**C**) or MM1.S (**D**) cells (mean and SEM, \* p<0.05, \*\* p<0.01, \*\*\* p<0.001, \*\*\*\* p<0.0001, one-way ANOVA), n=3, 2 replicates. **E-G**, The head-to-head comparison of single BCMA-CART and dual BCMA-SLAMF7-CART in an OPM-2 xenograft mouse model. NSG mice were injected with 1x10<sup>6</sup> of luciferase<sup>+</sup> OPM-2 cells on day -28. On day -1, tumor burden was assessed with bioluminescence imaging (BLI) and mice were randomized according to the tumor burden. On day 0, mice received 1x10<sup>6</sup> of 1) UTD, 2) BCMA-CART, or 3) BCMA-SLAMF7-CART (mean and SEM, \* p<0.05 at day 13, two-way ANOVA; n=5 per group). **G**, Kaplan-Meier curve of OPM-2 xenograft mouse model is shown [BCMA-CART vs. BCMA-SLAMF7-CART hazard ratio = 0.0630; 95% confidence interval (CI) = 0.005903-0.6722, \*p=0.05].

Supplemental Figure S22



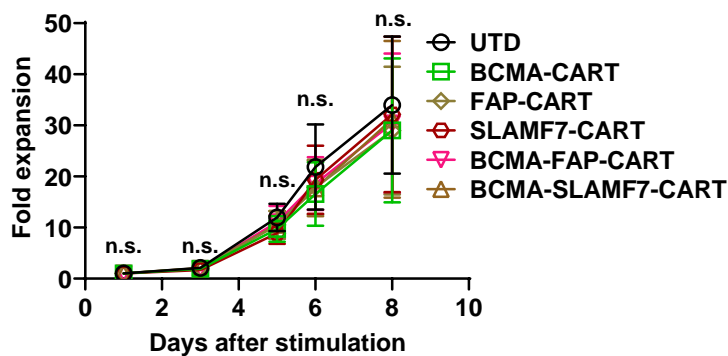
**Supplemental Figure S22 | Dual BCMA-SLAMF7 targeting CART cells overcome BM-CAF-induced impairment of BCMA-CART killing.** UTD, BCMA-CART, or BCMA-SLAMF7-CART-cells were co-cultured with Luciferase positive OPM-2 cells at different E:T ratio, in the presence or absence of BM-CAFs (ratio of OPM-2: CAFs of 1:0.1; at 0.6:1 ratio, mean and SEM, \* p<0.05, \*\* p<0.01, one-way ANOVA); n=3, 2 replicates.



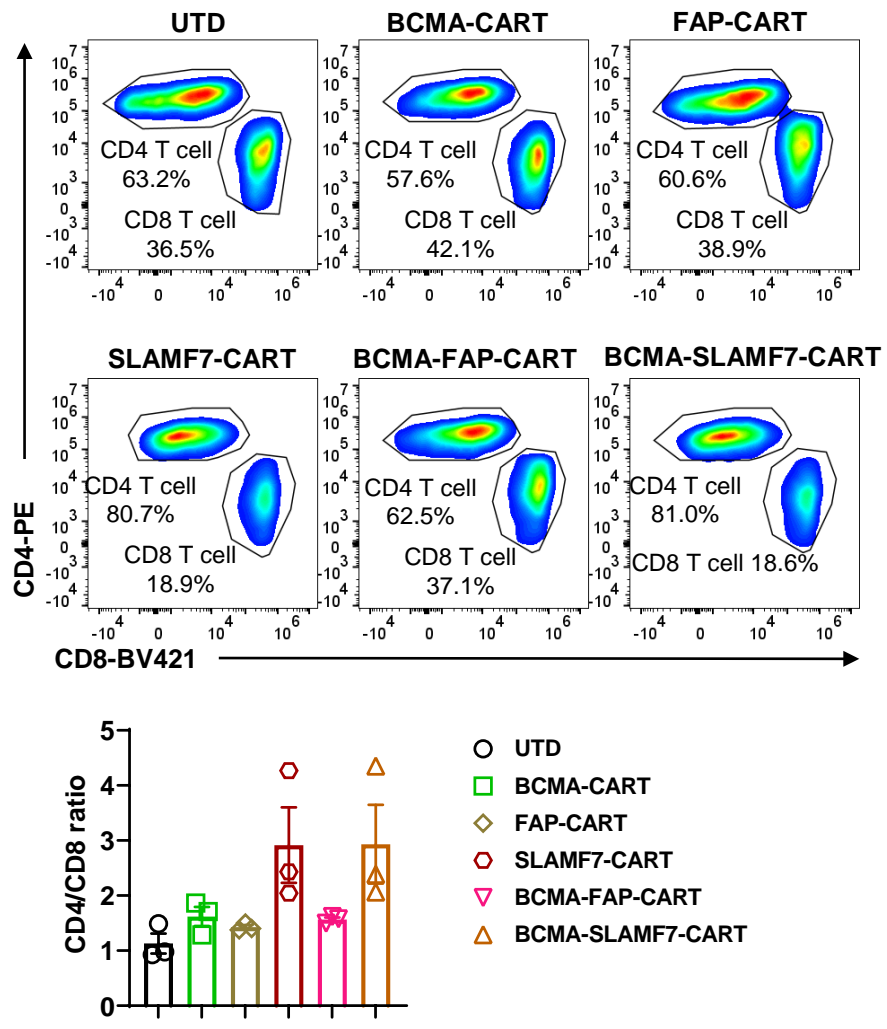


**Supplemental Figure S23 | BCMA-SLAMF7- or BCMA-FAP-CART demonstrate a long-term durable response and improve overall survival in the MM-TME mouse model.** **A**, Experimental schema. Three weeks after the injection of 1x10<sup>6</sup> luciferase<sup>+</sup> MM1.S and 1x10<sup>6</sup> BM-CAFs, mice were randomized into four groups: 1) UTD, 2) BCMA-CART, 3) BCMA-SLAMF7-CART, or 4) BCMA-FAP-CART. Tumor burden was assessed by BLI (3 mice per group). **B** and **C**, Bioluminescent imaging of mice treated with UTD or CART (mean and SEM, \*p<0.05, two-way ANOVA at day 27). **D**, Kaplan-Meier survival curve is shown. [BCMA-CART vs. BCMA-SLAMF7-CART hazard ratio = 0.06518; 95% confidence interval (CI) = 0.006025 to 0.7051, \*p=0.02, BCMA-CART vs. BCMA-FAP-CART hazard ratio = 0.06518; 95% CI = 0.006025 to 0.7051, \*p=0.02].

A



B



**Supplemental Figure S24 | CART-cell expansion and the composition of CART at day 8 of the generation.** A, T cells were isolated from the healthy-donor-derived PBMCs. T cells were then stimulated with anti-CD3/CD28 beads at 1:3 (T cells:beads). CARs were lentivirally transduced on day 1 at an MOI of 3. T cells were counted on days 0, 3, 5, 6, and 8. Beads were removed from T cells on day 6. B, Representative flow plots of UTD, BCMA-, FAP-, SLAMF7-, BCMA-FAP-, and BCMA-SLAMF7-CART-cells (n=3).